FLEXURAL PERFORMANCE OF CONCRETE BEAMS REINFORCED WITH BASALT FIBER REINFORCED POLYMERS (BFRP) BARS

by

Mustafa Adel Muhsin Al-Mimar

A Thesis Presented to the Faculty of the
American University of Sharjah
College of Engineering
in Partial Fulfillment
of the Requirements
for the Degree of

Master of Science in
Civil Engineering

Sharjah, United Arab Emirates

May. 2019

Approval Signatures

We, the undersigned, approve the Master's Thesis of Mustafa Adel Muhsin Al-Mimar

Thesis Title: Flexural Performance of Concrete Beams Reinforced with Basalt Fiber Reinforced Polymers (BFRP) Bars

Signature	**Date of Signature** (dd/mm/yyyy)
_____	_____
Dr. Farid Abed Professor, Department of Civil Engineering Thesis Advisor	
_____	_____
Dr. Rami Haweeleh Professor, Department of Civil Engineering Thesis Committee Member	
_____	_____
Dr. Basil Darras Associate Professor, Department of Mechanical Engineering Thesis Committee Member	
_____	_____
Dr. Irtishad U. Ahmad Head, Department of Civil Engineering	
_____	_____
Dr. Lotfi Romdhane Associate Dean for Graduate Affairs and Research College of Engineering	
_____	_____
Dr. Naif Darwish Acting Dean, College of Engineering	
_____	_____
Dr. Mohamed El-Tarhuni Vice Provost for Graduate Studies	

Acknowledgements

I would like to express my truthful appreciation and gratitude to my supervisor Dr. Farid Abed for his continuous support during my master's thesis, his patience, encouragement and guidance.

Many thanks as well to the College of Engineering, Department of Civil Engineering at the American University of Sharjah for providing me with the part time teaching assistant program during my postgraduate studies.

Many appreciations to Mr. Arshi Faridi – construction materials lab instructor and Mr. Waleed Nawaz for their help and guidance in conducting the test in the lab. I would like to thank the construction materials laboratory technician Mr. Mohammed Ansari for helping me in setting the experimental setup for testing the beams and providing me with all the equipment needed.

Special thanks to Mr. Abu Bakr Mohammed – for his help in testing and conducting the experiments in the laboratory.

Dedication

This thesis is dedicated to

my lovely family and wife

Abstract

This research studies the flexural behavior of concrete beams that are reinforced longitudinally with the newly discovered Basalt Fiber Reinforced Polymers (BFRP) bars. The aim is to examine the suitability of using BFRP bars in flexure as compared to Carbon FRP bars and to validate its compatibility with the recommendations and guidelines of the current ACI440 Code. The effect of different design parameters such as BFRP reinforcement ratio, reinforcement axial stiffness and concrete compressive strength are studied. In addition, this research sheds the light on evaluating the bond-dependent coefficient (k_b) value for this new type of FRP composites. Four-point loading tests were performed on a total of 14 beams (180 mm × 230 mm × 2200 mm) to achieve the objectives of this research. The loads vs mid-span deflections, cracks behavior and widths, ultimate capacities and failure modes of all 14 beams are recorded and discussed. Results confirmed that BFRP bars could be a valuable alternative to steel and CFRP bars and can be used in similar applications in the construction industry. The flexural behavior of BFRP-reinforced beams compared well with the ACI440.1R guidelines. The experimental moment capacities well-matched their theoretical counterparts using the code equations. For all the beams, the calculated bond dependent coefficients (k_b) values were found to be lower than the values recommended by the ACI440.1R code which clearly indicates a strong bond between the FRP bars and concrete. The test results can be utilized as a control for a long-term durability study on the performance of BFRP bars under the harsh environment.

Search Terms: ***Flexure, BFRP bar, CFRP bar, bond-dependent coefficient (k_b), Axial Stiffness (EA)***

Table of Contents

List of Figures

List of Tables

Chapter 1: Introduction

Fiber Reinforced Polymers (FRP) material is becoming more common in the engineering practices. Engineers are being attracted by FRP materials as a better substitute for reinforcing steel. FRP is defined in the ACI 440 as a “composite materials consisting of continuous fibers impregnated with a fiber binding polymer then molded and hardened in the intended shape " [1]. The most common FRP materials are carbon FRP (CFRP), Aramid FRP (AFRP) and Glass FRP (GFRP). Most recently a new FRP material made of basalt (BFRP) has emerged. FRP materials are available in different forms, such as bars, sheets and plates. Thorough Studies have been conducted on CFRP and GFRP materials. On the other hand, BFRP materials are in the state of ongoing research since they have newly emerged in the engineering industry. This research focuses on studying the flexural behavior of concrete beams reinforced with BFRP bars compared to concrete beams reinforced with CFRP bars and conventional steel.

FRP materials have many advantages that make them pull the attention of civil engineers to consider using them in reinforced concrete structures as an alternative to conventional steel. They are non-corrosive materials that can resist cruel environmental conditions that damage conventional steel with time, have low densities and high strength to weight ratio compared to the usual steel reinforcement. As a result, BFRP have low transportation cost and they are easy to handle due to its light weight. As per ACI 440, "FRP bars have a density ranging from 1.25 to 2.1 g/cm^3 which is one-sixth to one-fourth that of steel". With respect to the tensile behavior, the behavior of FRP composites is different than steel. FRP materials go through full elastic behavior that ends with failure without going through any ductile behavior as in steel, as shown in Figure 1.

As per the United Arab Emirates market, FRP composites are commonly used in repair and strengthening works, whereas, steel rebar is the most favorable reinforcing material that is used in new construction works. For the 12 mm dimeter, the price of Carbon FRP bars is approximately 100 AED per linear meter while the costs of Glass and Basalt bars cost are around 15 and 10 AED per linear meter, respectively. On the other hand, steel bars (12mm diameter) cost around 2 AED per linear meter. Although FRP bars are more expensive than steel bars, the FRP-reinforced concrete structures are

expected to have longer life spans than conventional steel-reinforced concrete structures considering the corrosion problems under the UAE harsh environment.

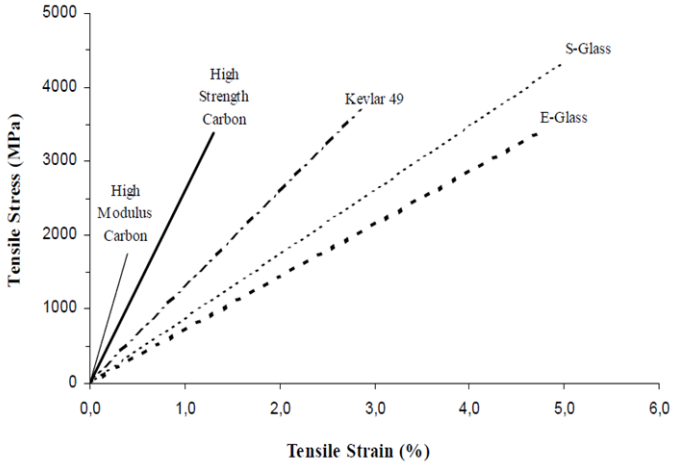

Figure 1: Stress-strain curve for different FRP composites [2]

Many factors affect the behavior of the FRP materials. The ratio of the fibers volume fraction to the total volume of the composite predict the tensile behavior of the composite. Moreover, according to ACI440, the mechanical properties of the FRP materials are significantly affected by the curing rate and the quality control of the manufacturing process [1]. The coefficient of thermal expansion of FRP composites varies between the longitudinal direction and the transverse direction. In the longitudinal direction, it is mainly affected by the properties of the fibers. In the transverse direction, it is mainly affected by the type of the resin. Table 1 displays the mechanical properties of the commonly used FRP materials compared to conventional steel.

Similar to carbon fibers, basalt fibers are produced through the melting process of the naturally molten volcanic rocks [3]. Basalt fibers contain natural raw materials which make it cost effective material compared to carbon fibers. It is a nontoxic material, environmental friendly and corrosion resistant. Similarly, basalt fibers are magnetic insulators and have high fatigue resistance. Recent studies are being conducted on BFRP bars to replace the conventional FRP materials (CFRP, GFRP and AFRP) as main reinforcement in reinforced concrete structures. Besides, BFRP materials are durable and can resist harsh environmental conditions.

Table 1: Mechanical properties of FRP bars According to ACI440 committee [1]

	Steel	GFRP	CFRP	AFRP
Nominal yield stress (MPa)	276 to 517	N/A	N/A	N/A
Tensile strength (MPa)	483 to 690	483 to 1600	600 to 3690	1720 to 2540
Elastic modulus (GPa)	200.0	35.0 to 51.0	120.0 to 580.0	41.0 to 125.0
Yield strain %	0.14 to 0.25	N/A	N/A	N/A
Rupture strain %	6.0 to 12.0	1.2 to 3.1	0.5 to 1.7	1.9 to 4.4
Density (g/cm^3)	7.90	1.25 to 2.10	1.50 to 1.60	1.25 to 1.40
Longitudinal	11.7	6.0 to 10.0	-9.0 to 0.0	-6.0 to -2.0
Transverse	11.7	21.0 to 23.0	74.0 to 104.0	60.0 to 80.0

It is essential to study the bond of the reinforcing material with concrete. To achieve high capacities, the bond between the reinforcement and the concrete must be high. Not only the capacity, the bond is also critical in determining the anchorage of the bar, crack distribution and serviceability. A good bond between the reinforcing bars and the concrete indicates a long-life span of the structure which also leads to a more durable structure. The bond of the FRP bars with concrete is different to that of steel. The bond of steel bars with concrete is mainly affected by the shear strength of the concrete. Researchers are studying the bond of the BFRP bars with concrete. Furthermore, studies are conducted to explore the bond strength of the BFRP bars with concrete under harsh environmental conditions.

1.1 Problem Statement

With the increased demand of the newly emerging construction material, studies are increasing on those materials to examine their effectiveness on the structural performance. Studies have shown that steel bars are subjected to corrosion when placed in concrete. When steel bars corrode, concrete section cracks causing failure. Once the steel bars corrode, special repair methods and techniques need to be applied to restore the capacity of those bars. Repair methods are time consuming and expensive. The

newly developed BFRP bars are high strength anti-corrosion materials. In this research, different sizes of BFRP bars will be examined when used as longitudinal reinforcement in concrete beams. Eight concrete beams longitudinally reinforced with Basalt FRP bars are tested in flexure and compared to four concrete beams reinforced with steel bars and two concrete beams reinforced longitudinally with Carbon FRP bars. Moreover, The ACI440 committee recommends a bond-dependent coefficient (k_b) default value of 1.4 to calculate crack width for new FRP material [1]. The proposed research aims to tackle this conservative recommendation with experimental results so that it can be reduced.

1.2 Research Significance

The significance of this research is to study and investigate the newly emerged BFRP bars as a viable alternative reinforcement in structural concrete members. This research examines the flexural performance of the BFRP bars in reinforcing concrete structures compared to FRP bars made of carbon and conventional steel bars. The evaluation of the bond-dependent coefficient (k_b) of the BFRP bars is also part of this study. The behavior of different sizes of the newly developed sand-coated BFRP bars is investigated in different aspects. In addition, two different concrete mixes with normal and high compressive strengths will be used for comprehensive understanding. The results will be utilized to provide recommendations to the ACI Committee to adopt the new BFRP bars in the ACI440 guidelines.

1.3 Research Objectives

Since BFRP is a newly revealed material, few researches have been conducted on this material. Many researches focused on the mechanical properties of the BFRP including the tensile properties and the bond with concrete. This research aims to add to the literature some experimental results on the flexural performance of BFRP bars as the main reinforcement in structural concrete members. The objectives of this research are summarized as follows:

1. To study the flexural behavior and serviceability performance of concrete beams reinforced with newly developed sand-coated BFRP bars of different sizes. The aim is to understand the flexural response in terms of, moment capacity, mode of failure, cracking patterns and deflection.

2. To evaluate the bond-dependent coefficient (k_b) for the sand-coated BFRP bars in order to provide recommendations to the ACI committee of the bond-dependent factor (k_b) values that may be used for this new type of FRP bars.
3. To study the effect of concrete compressive strength on the overall flexural behavior of concrete beams reinforced with BFRP bars by considering two different concrete mixes, normal and high strength.
4. To compare the performance of BFRP-RC beams with CFRP-RC and steel-RC beams.

1.4 Thesis Structure

This thesis is divided into several chapters that serve the purpose of this research. After the abstract, the thesis starts with the introduction chapter which enlightens the reader by describing the use of several types of FRP bars along with steel bars. The first chapter also states the problem statement and the objectives of this research. The second chapter presents the outcomes of previous studies that have been done by other researchers on different FRP composites including BFRP. Chapter 3 explains the experimental setup and the procedure used in this research. In addition, it presents the testing matrix and materials along with instruments that have been used. Chapter 4 summarizes all the results from the experimental test. The cracking behavior, maximum load and deflection are displayed in the same chapter. Chapter 5 explains the design considerations for FRP-reinforce concrete beams as per ACI440 guidelines. In the sixth chapter, the results obtained are discussed and processed. The comparison between all types of beams are carried out in chapter 6. Chapter 7 highlights the results and conclusions of this research. Furthermore, it captures all the key points of this study along with recommendations for future researches.

Chapter 2: Literature Review

2.1 Background on Fiber Reinforced Polymers (FRP) Composites

Fiber Reinforced Polymer (FRP) materials are manufactured to produce a synergistic material [2]. Using a polymeric resin and small-diameters fibers, these kinds of materials are combined at microscopic level making it one of the most commonly used materials in the construction industry over recent years. Having a high tensile strength and being lightweight are the most attractive features of the FRP materials. Moreover, its nonconductive behavior and high corrosion resistance made these materials more desirable by engineers. These features make the FRP material the first option that any structural engineer will think of not only in strengthening structural elements but also in designing new concrete members. Numerous studies have been conducted on FRP composites and steel bars to understand its behavior, see (Alhamad et al. [4], Altalmas [5] and Abedi [6].

2.2 Fiber Reinforced Polymers (FRP) Forms

The FRP composites have been used in wide range of application in several fields including water retaining structures, airports and bridges. Various FRP composites are used extensively in structures that are exposed to harsh environment. According to Columbia et al. [7], FRP composites are manufactured through a process called pultrusion. It generates prismatic thin elements by continuous manufacturing process. FRP composites can be in a form of fibers, sheets, bars or plates. The most common types of FRP composites are sheets and bars which are widely used in structural elements. They can be embedded internally in the structural elements as main reinforcement, or they can be bonded externally to strengthen an existing structural element. FRP composites are brittle and tend to break when reaching the ultimate load carrying capacity.

2.3 The Bond of Fiber Reinforced Polymers (FRP) Bars

The bond of FRP bars is the main characteristic that distinguish FRP material from other conventional materials like steel. According to several studies, FRP bars showed good bond to concrete. In addition, Rafi et al. [8] stated that the development length of the bar affects its bond strength. As per ACI440, the bond of longitudinally reinforcing FRP bars must be fully developed to avoid failure caused by bar slip [1].

The development length of FRP bars vary between 26 to 37 times the bar diameter depending on the FRP material.

2.4 Carbon and Glass Fiber Reinforced Polymers (CFRP, GFRP)

Many studies have been conducted on Fiber Reinforced Polymers bars, Carbon FRP, Glass FRP and Basalt FRP. Abed et al. [9] studied the shear characteristics of concrete deep beams reinforced with GFRP bars and without web reinforcement. A four-point load test was conducted to a total of 13 beams until failure; nine beams were reinforced with Glass FRP bars and four beams were reinforced with conventional steel bars. The purpose of the study was to investigate the effect of shear span to depth ratio (a/d) on the ultimate shear capacity of the beams. In addition, the effects of the reinforcement ratio, the concrete compressive strength and the effective depth of the beam (d) were investigated. The study showed that the GFRP reinforced beams experienced higher deflection at mid-span than the steel reinforced beams, due to the low modulus of elasticity of the GFRP bars. As a result, the beams reinforced with GFRP bears exhibited wider cracks and lesser aggregate interlock. Besides, the low modulus of elasticity led to lower dowel action presented in the GFRP reinforced beams. The study reported that increasing the reinforcement ratio improved the shear strength but not significantly.

In (1998), Theriault et al. [10] inspected how the flexural behavior of beams that are reinforced with FRP bars is affected by the main reinforcement and concrete strength. A flexural test was conducted on twelve beams reinforced longitudinally with GFRP bars. The study reported that the crack spacing was negligibly affected by the main reinforcement ratio and the compressive strength of concrete. In addition, the study conveyed that when the reinforcement ratio increased, the crack width values decreased.

In 2015, El refai, Abed and Al-Rahmani [11] investigated the perforcmance and serviceacility of Glass FRP reinforced concrete beams and steel reinforced concrete beams. Six beams reinforced with GFRP and steel bars were tested in flexure. The study showed that using GFRP bars along with steel bars enhanced the behavior of the concrete beams in terms of load carrying capacity, cracking stiffness and deformability. The study recommended that steel yielding shall be considered prior to crushing of

concrete or rupturing of the FRP bars when designing hybrid-reinforced beams. The study reported that all hybrid-reinforced beams failed in steel yielding followed by concrete crushing.

Sagher et al. [12] has done a parametric study in (2017) on the shear behavior of short concrete beams that are reinforced with GFRP bars. The purpose of the study was to investigate the effect of different parameters including the reinforcement ratio, beam's span to depth ratio and beam's height on the shear strength of GFRP-reinforced beams. The study reported a 33% increase in shear strength when the reinforcement ratio of the beams increased from 0.26% to 1.64%. The study claimed that the increase in the shear capacity is due to the contribution of the GFRP bars in resisting the shear load as a tension tie. In addition, the study showed that increasing the beam's height by 12.5% led to a 22% increase in the shear strength as a result of the arch-action mechanism. Moreover, the study reported that decreasing the span to depth ratio increased the shear strength of the beams.

A study done by Habeeb et al. [13] investigated the flexural behavior of GFRP-reinforced continuous concrete beams. The main parameter of the experimental program of the study was the reinforcement ratio. A total number of five beams were tested in the study; two beams were simply supported, and three continuous beams reinforced with GFRP bars. For comparison purposes, one concrete beam reinforced with steel bars was cast and tested in the study. Some of the beams were designed as over-reinforced with GFRP bars and some of them were under-reinforced in negative and positive moment regions. The first crack in the over-reinforced beams initiated at a higher load than in the under-reinforced beams at the middle of the span. In addition, the cracks originated at the hogging moment region in the over-reinforced beams. On the other hand, cracks propagated in the sagging moment region in the under-reinforced GFRP beams. According to the study [13], the under-reinforced beams failed in FRP rupture. In contrast, the over-reinforced GFRP beams failed in concrete crushing. In addition, concrete failure along with shear failure was reported as a third mode of failure in the concrete beams that are over-reinforced with GFRP bars. The study justified that the compression resistance in the over-reinforced GFRP beams was very high which altered the mode of failure to be dominated by shear. The outcomes of the study showed that the ultimate load of the continuous over-reinforced GFRP beams was higher by

50% than the simply supported over-reinforced GFRP beams. Similarly, the continuous under reinforced GFRP beams failed at a 40% higher load than the simply supported under reinforced GFRP beams.

Another research was done by Zhang et al. [14] studied the bond failure of the near surface mounted FRP bars and concrete. The study was done on 23 beams strengthened with NSM-FRP bars. The forms of failure observed were splitting of the epoxy adhesive, local deboning caused by concrete cracking, and FRP rupturing. Moreover, the FRP bars enhanced the flexural capacities of the strengthened beams. It was noticed that at low level of loading, steel yielding and crack propagation led to a nonlinear strain distribution along the bonded length of the bar. However, "at ultimate, the strain varies almost linearly along the bonded length, which means that the bond stress has gradually transferred from the loaded end to the free end till it to be a constant value throughout" [14].

A research conducted by Abdul-Salam et al. [15] studied the shear resistance of one-way slabs reinforced with FRP bars. Shear test was performed to sixteen concrete slabs that were reinforced with CFRP and GFRP bars. The slabs failed in sudden and brittle shear failure. The CFRP-reinforced slabs collapsed into two separate parts which is an undesirable mode of failure. Whereas, GFRP-reinforced slabs showed more desirable modes of failure which indicated that they maintained their integrity after failure [15]. In addition, according to the study, increasing the compressive strength of the concrete increased the shear capacity of the slab to a certain point, further increase in compressive strength negatively affected the slab shear capacity.

Another study by Calvet et al. [16] analyzed the effect of the environmental conditions on the bond of different CFRP bars in comparison to steel bars. The study claims that the sanded CFRP bars showed the best bond behavior which is 10 % greater than steel bars. Besides, the shear stress of the CFRP ribbed bars was as high as that of ribbed steel bars. The deformed and the textured bars failed due to shear of concrete in the grooves under all conditions of the study. At high temperatures, the textured layer was separated from rest of the bar. Although there are discrepancies between the theoretical and experimental values, the design guides do not differentiate between the diverse types of CFRP bars in calculating the bond strength.

Escórcio et al. [17] did an experimental study about rehabilitation, using GFRP bars instead of steel bars of reinforced concrete beams. The aim of the study is to find an alternative to replace steel bars in retrofitting damaged structures. According to Escórcio et al. [17], the concrete beams were casted in two stages to simulate the cracked concrete. The result of the study is that the rehabilitated beams with GFRP bars showed a bilinear behavior until failure in terms of load-deflection since the ductile performance of the original damaged beam with steel reinforcement is not possible to reproduce due to the GFRP material linear elastic property.

El-Nemr et al. [18] studied the bond-dependent (k_b) factor of the glass and carbon FRP bars in normal and high strength concretes. The study aimed to investigate the k_b values of sand-coated and helically grooved GFRP bars and sand-coated CFRP bars in normal and high strength concretes. According to El-Nemr et al. [18], the sand-coated GFRP bars showed smaller k_b than the helically grooved GFRP bars. The calculations of k_b values were determined at crack widths = 0.7 mm. The study recommends that the design should be done based on experimental testing of the material rather than theoretical values. The k_b values ranged between 0.8 and 1, however, the ACI 440 committee recommends a k_b value of 1.4.

A research done by Tamimi et al. [19] investigated the effect of severe environment exposures on the bond between concrete and the GFRP bars. 12 GFRP bars and 4 steel bars samples were tested under direct pullout after being exposed to sea water splash and direct sun. The study stated that between 60 and 90 days exposures, there was no substantial difference on the bond strength. Moreover, the study asserts that the ACI 440.1R-06 equation of calculating the bond stress is conservative.

2.5 Basalt Fiber Reinforced Polymers (BFRP)

Recent studies are concentrating on the newly revealed fiber reinforced polymers made of Basalt (BFRP). When compared with GFRP, BFRP materials are more chemically stable. In addition, they have higher tensile strength and modulus of elasticity. Moreover, BFRP composites have much lower cost in comparison to CFRP. Having all the previous advantages, BFRP composites are anticipated to be the one of the desired materials by engineers that can be used in structural strengthening as well as new construction.

Up to date, very few studies have been conducted on BFRP materials. The flexural response of Basalt FRP reinforced concrete beams was studied by Abed et al. [20]. The beams were cast with fiber reinforced concrete. The main purpose of the study is to examine how different lengths of basalt fibers affect the performance of BFRP-reinforced beams. The study showed that the moment capacity of the BFRP-reinforced beams was enhanced by adding Basalt fibers to the concrete. The study stated that introducing Basalt fibers to the concrete improved the concrete compression strain which assisted the BFRP bars to contribute more in resisting the applied loads. In addition, the flexural capacity of the BFRP-reinforced beams has increased by increasing the reinforcement ratio. The increase in the capacity followed similar trend of the ACI440.1R-15 moment capacity equation. Moreover, the study reported that when the reinforcement ratio in kept constant, the curvature ductility and the cracking behavior were improved in the beams with more number of bars.

A research by El Refai et al. [21] studied the shear behavior of concrete beams that are reinforced with BFRP bars. Ten BFRP-reinforced concrete beams were tested with no transverse reinforcement and compared with 75 FRP-reinforced beams from previously conducted studies in the literature. Almost all the tested beams failed in shear with diagonal tension cracks along with splitting. The study reported that the concrete shear capacity (V_c) decreases as the span to depth ratio (a/d) increases. The study stated that increasing the longitudinal reinforcement ratio increased the concrete shear strength (V_c). The study concluded that the shear behavior of the tested BFRP-reinforced beams is close to other FRP-reinforced beams.

In (2015), El Refai, Abed and Altalmas [22] studied the effect of different environments on the bond durability of the FRP bars made of Basalt and Glass. The bars were exposed to harsh environment such that, sea water, tap water and elevated temperature. As per the study, the BFRP and GFRP bars failed in pullout, where the bar layers failed in interlaminar shear in the BFRP bars and the shearing of the glass ribs for the GFRP bars [22]. The study reported the surface texture of the bar controlled the bond stress response. For the BFRP, the sand-coated bars showed better bond strength than the grooved bars. The research stated that exposing the bars to the elevated temperature had a negligible effect on the FRP bars. after immersing the bars in an

aqueous solution, the bond strength reduction was governed by percentage of moisture absorption.

Altalmas et al. [22] have studied the bond degradation of BFRP bars exposed to accelerated aging conditions. Direct pullout tests have been done to sixty-two sand-coated and ribbed BFRP and GFRP bars. The study showed that sand-coated bars observed higher bond to the concrete than the ribbed bars regardless of the fibers type. Furthermore, the study confirmed that BFRP bars can be used as reinforcing material. Dong et al. [3] examined the durability of the bond of Basalt FRP bars embedded in concrete under sea water. They predicted the long-term bond strength of different FRP and steel bars. The research proved that the sand-coated BFRP bars have higher bond durability than ribbed bars but lower bond strength. Moreover, the study pointed out that the ribbed FRP bars have higher bond strength than conventional steel bars.

Hassan et al. [23] studied the bond durability of BFRP bars in concrete beams when exposed to harsh environment. The specimens were immersed in alkaline solution with elevated temperature. All the specimens failed in pullout mode of failure by slipping through the free end; the mode of failure was dominated by shear. Hassan et al. [23] concluded that the bond strength increased by increasing the temperature. A 25% increase in bond strength was noticed during the study by increasing the temperature from 50º to 60ºC.

Elgabbas et al. [24] studied the physical and mechanical properties of BFRP bars for reinforcing concrete structures. They studied the behavior of BFRP bars in alkali condition. They claimed that the characteristics of BFRP type A bars (for pre-stressing) comply with the conventional pre-stressing steel tendons. “The strength degradation observed in the BFRP bars was attributed to the fiber–matrix interface (sizing), which evidenced poor bonding between the resin and basalt fibers” [24]. They recommended further investigations for BFRP bars in order to generate confidence and to be accepted in the industry.

Another research was done by Elgabbas et al. [25] about testing the BFRP bars in concrete beams. This experimental study aimed to determine the bond dependent coefficient (k_b) and investigating the structural performance of newly developed sand-coated BFRP bars in normal strength concrete beams [25]. A four-point load bending

test has been conducted on six beams (200 mm × 300 mm) and 3100 mm in length with different BFRP bars diameter. The average bond-dependent coefficient (k_b) was determined using the first three cracks in each beam and was estimated around 0.76 ± 0.03 for the BFRP bars with sand-coated surface. Benmokrane et al. [25] stated that the general behavior of concrete beams reinforced with BFRP bars is affected by the axial stiffness of the reinforcement. The performance of the tested beams was improved in terms of lower deflection, lower strain, and lower crack width at the same load level, at higher axial stiffness.

Tomlinson et al. [26] studied the flexural and shear performance of concrete beams that are reinforced with Basalt FRP bars. A four-point bending test has been performed to nine beams that were reinforced with different reinforcement ratios of BFRP bars. Tomlinson et al. [26] stated that the ultimate load capacities of the beams are directly related to the reinforcement ratio regardless of the failure mode. Failure by stirrups rupture was reported in the beams that are reinforced with BFRP stirrups. The study stated that by increasing the reinforcement ratio, the moment capacities of the beams increased. A study by Wang et al. [27] investigated the ductility of fiber-reinforced concrete beams that are reinforced with FRP bars. The study reported that the crack width values were smaller in the fiber reinforced concrete beams. In addition, the FRC beams reached higher concrete strains than the beams that were cast with plain concrete. According to the study, adding fibers to the concrete enhanced the ductility of the beams by 40%.

In (2015), El Refai et al. [28] investigated the bond performance of BFRP bars to concrete. Direct pullout test was performed to thirty six concrete cyliders that were reinforced with BFRP bars and twelves GFRP-reinforced concrete cylinders. The study reported that the BFRP bars exhibited 75% bond strength of that of GFRP bars. At the initial loading stage, BFRP bars with small diameters showed better bond to concrete. Moreover, the study stated that the BFRP bars showed higher residual stresses values than that of GFRP bars. Several finite element studies have been done to simulate the behavior of the FRP composites and compare with the experimental and the theoretical one, see (Abed et al. [29], El Refai et al. [30], Abed et al. [31], Abed et al. [32], Al-Rahmani et al. [33] and Makarem et al. [34]).

The key purpose of this research is to investigate the flexural behavior of the newly discovered BFRP bars when used as main reinforcement in concrete beams. This research will study the deflection and cracking behavior, cracking patterns, crack width values and the strain in FRP reinforcement as well as in the concrete. In addition, the bond dependent coefficient (k_b) value is inspected as well. The testing setup and procedure are proposed to be able to measure the required values and present accurate results for this research. All beams are subjected to a four-point load until failure. The testing matrix is proposed to compare the results obtained from the BFRP-reinforced beams and compare it with the results of steel and CFRP-reinforced beams.

Chapter 3: Experimental Program

This chapter discusses the experimental program which includes the material properties, beams configurations, testing setup and considerations that are followed in this research.

3.1 Material Properties

3.1.1 Basalt fiber-reinforced polymer (BFRP) bars. The key objective of this research is to study the flexural behavior of concrete beams that are reinforced with BFRP bars. The BFRP bars are supplied from Galen, a company which manufactures FRP products in Russia. The elastic modulus of BFRP bars ranges from 42.6 to 46.6 GPa for different bar diameters. The values of the ultimate tensile strength are between 1028 to 1121 MPa for the tested bars, as per the manufacturer specifications. To study the behavior of BFRP bars in concrete beams, different bar sizes including 8, 10, 12 and 16 mm are used as main longitudinal reinforcement. The texture of the BFRP bars is sand-coated which increases the bond between the BFRP bar and concrete. Figure 2 shows a sample photo of the BFRP bars used in this research.

Figure 2: A sample of sand-coated BFRP bars used in this study

3.1.2 Carbon fiber-reinforced polymer (CFRP) Bars. In this research, two beams reinforced with two carbon FRP bars are considered for comparison purposes. The CFRP bars are manufactured and supplied by Structural Technologies LLC in the United States. As per the manufacturer's data sheet, the ultimate tensile strength of the CFRP bars is 2068 MPa and the modulus of elasticity is 131 GPa. The ultimate tensile strain of the Carbon FRP bars is 1.58%. Similar to the BFRP bars, the texture of the CFRP bars is sand-coated to enhance the bond between the bars and concrete. Figure 3 shows a photo of the 12 mm diameter CFRP bar that is used in this study.

Figure 3: A sample of sand-coated CFRP bar used in this study

3.1.3 Steel Reinforcement Bars. Steel bars of diameters 10mm and 12mm are used as flexural reinforcement in the beams, refer to Figure 4. The steel bars have yield strength of 460 MPa and a typical modulus of elasticity of 200 GPa. Four beams reinforced with steel bars are utilized for comparison purposes.

Figure 4: A sample of ribbed steel bars used in this study

Table 2 gives a summary of the mechanical properties of BFRP, CFRP and steel bars used in this study. Tensile tests for all BFRP bars were conducted to verify the ultimate tensile strength and the elastic modulus values given by the manufacturers.

Table 2: Mechanical Properties of BFRP, CFRP and Steel Bars

Type	Nominal Diameter (mm)	Cross-sectional Area (mm^2)	Ultimate Tensile Strength (MPa)	Ultimate Tensile Strain (%)	Elastic Modulus (GPa)
CFRP*	12	113	2068	1.58	131
BFRP	8	57.4	1075.1±37	2.1±0.1	42.9±1.4
	10	58.4	1028.7±47	2.4±0.1	42.8±1.3
	12	121.3	1118.6±31	2.4	46.6±1.7
	16	211.9	1121.3±56	2.4	46±2.1
Steel*	10	78.5	460	0.23	200
	12	113			

* As per the manufacturer

3.1.4 Concrete mix. Two different concrete mixes are used in this study, Normal Strength Concrete (NSC) and High Strength Concrete (HSC). The target concrete compressive strengths are 30MPa for the NSC and 60MPa for the HSC. The concrete is provided by SAFE mix, a concrete plant in Sharjah, UAE. Table 3 presents the unit weights of different concrete components for both mixes. The mix 30-20 OPC has a water cement ratio (W/C) of 0.48 and a total unit weight of 2415 Kg/m3. On the other hand, the mix 60-20 OPC+MS has a lower w/c ratio of 0.36. Moreover, 40 Kg/m3 of Micro silica, a chemical admixture used to increase the compressive strength, is added to 60-20 OPC+MS mix. The beams are cast by SAFE mix concrete plant. The formwork of the beams was removed after 48 hours from casting. Moreover, curing using cloth sheets was done for a period of seven days. Figure 5 demonstrates the beams before and during casting of concrete. The reinforcement in terms of top bars, stirrups and bottom bars are placed inside the form work as per the details of the beams. The reinforcement strain gauges were installed at the midspan of the beam to record the strain in the reinforcement. Table 3 present the mix design of the two concrete mixes that were used as provided by the concrete supplier. The mix designs are done to ensure achieving the required compressive strengths.

(a) (b)

Figure 5: (a) beams before casting, (b) beams during casting

Table 3: Concrete Mix Design

Concrete Mix	Unit Weight (Kg/m^3)							
	Cement	Water	3/4" Aggregate	3/8" Aggregate	3/8 Sand	Dune Sand	Add-itive	Total Unit Weight
30-20 OPC	350	168	518	420	640	314	5	2415
60-20 OPC + MS	430	153	459	420	643	284	47.5	2436.5

The concrete cubes samples were tested in compression after 28 days to ensure that the desired strength has been attained. Table 4 shows the results obtained from the cubes compression test.

Table 4: Concrete Cubes results

Design Strength (MPa)	Cube Test Results (MPa)	Average value f_{cu} (MPa)	Average value f'_c (MPa)
30	46.7	47.5	38.0
	35.24*		
	48.24		
60	70.5	70.5	56.4
	72.3		
	68.6		

*Value is not considered in the calculation of the average value

3.2 Test Matrix and Specimens Configuration

The objective of this research is to study the behavior of BFRP bars as flexural reinforcement in concrete beams. To achieve the objectives of the research, a total of 14 beams are prepared to be tested in flexure. The beams are cast using two different concrete strength, high and normal. The beam's cross-section (180 mm × 230 mm) was selected such that it satisfies the ACI 440.1R-15 code [1] recommendations in terms of clear cover, bar spacing and number of bars that can be placed within the beam's width, minimum required depth (one tenth of the clear span) and to ensure slender specimen

with high span-to-depth ratio ($a/d \geq 3$). Figure 6 provides more details about the beams' cross-section adopted in this study.

The beams' dimensions and reinforcements are designed such that they fail in pure flexure rather than in shear or bar slip as illustrated in Figure 7. Stirrups of 10 mm diameter are provided each 100 mm over one-third of the span length (L/3) from each side of the beam to prevent shear failure. The span of the pure moment region with no shear reinforcement is set to 400 mm. The clear span of the beam is set to 1,900 mm with an additional 150 mm extension on each side of the beam, which makes its total length equal to 2,200 mm, to guarantee enough development length for FRP bars.

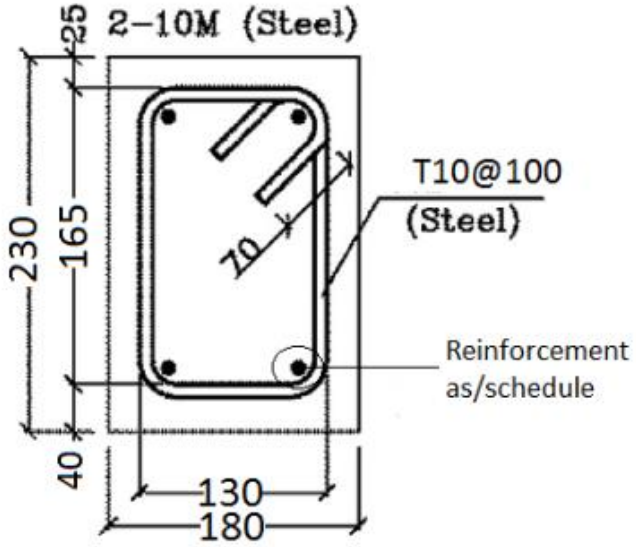

Figure 6: Beam's Cross-section

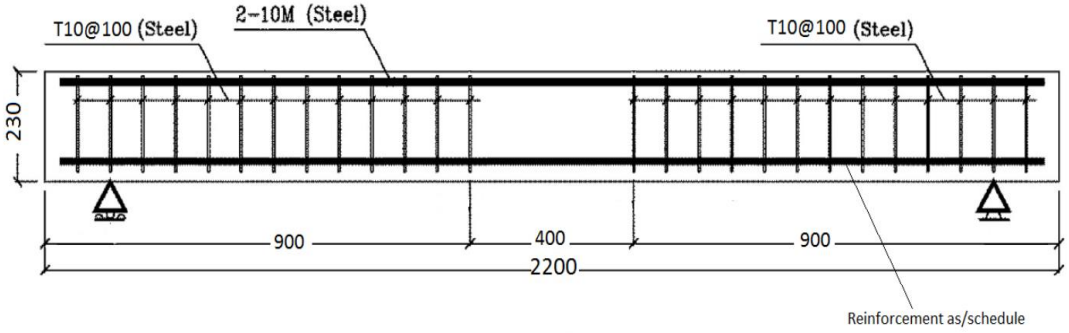

Figure 7: Beam's Elevation

Two sets of seven beams each were cast considering the normal and high concrete compressive strengths as listed in Table 5 and Table 6, respectively. The flexural test is conducted to study the performance of concrete beams reinforced with BFRP bars. The variables that are considered in the present test matrix include a) the effect of reinforcement type, b) the effect of reinforcement ratio, and c) the effect of concrete compressive strength. The effect of reinforcement ratios is studied by considering different BFRP bar numbers and diameters, such as No. 8, 10, 12 and 16 mm. In addition, the effect of reinforcement type aims to study the BFRP bars and compare it with the well-known reinforcing bars, namely steel and CFRP bars. Three beams are reinforced with the same reinforcement ratio but with different reinforcement type to examine the effect of reinforcement type on the performance of concrete beams. The designation of the beams is selected to represent the number of bars, bar type and concrete compressive strength. The first number denotes the number of the bottom reinforcement bars in each beam. The letter T and the second number represents the diameter of reinforcing bars in millimeters. The letters B, C and S indicate the reinforcing bar type which are BFRP, CFRP and steel, respectively. The last number denotes the concrete compressive strength of the beam. For example, the beam 3T8B-30 means that the beam is reinforced with 3 BFRP bars that are 8 mm in diameter and cast with 30 MPa concrete compressive strength.

Table 5: Summary of the experimental program – f'_c = 30 MPa

Beam ID	Number of Bars	Bar Size (mm)	Bar Type	ρ_{fb}	ρ_f / ρ_{fb}	Axial Stiffness EA (MN)
3T8B	3	8	BFRP	0.002353	1.90	7.5
2T10B	2	10	BFRP	0.00255	1.85	7.85
2T12B	2	12	BFRP	0.002352	2.90	11.3
3T16B	3	16	BFRP	0.00231	7.97	30.15
2T12C	2	12	CFRP	0.00183	3.73	29.6
2T10S	2	10	Steel	0.02911	0.16	31.4
2T12S	2	12	Steel	0.02911	0.23	45.2

Table 6: Summary of the experimental program – f'_c = 60 MPa

Beam ID	Number of Bars	Bar Size (mm)	Bar Type	ρ_{fb}	$\rho f/ \rho fb$	Axial Stiffness EA (MN)
3T8B	3	8	BFRP	0.0031	1.45	7.5
2T10B	2	10	BFRP	0.00336	1.4	7.85
2T12B	2	12	BFRP	0.0031	2.2	11.3
3T16B	3	16	BFRP	0.00305	6.03	30.15
2T12C	2	12	CFRP	0.0024	2.84	29.6
2T10S	2	10	Steel	0.0383	0.12	31.4
2T12S	2	12	Steel	0.0383	0.18	45.2

3.3 Test Setup and Instrumentation

A four-point loading setup shown in Figure 8 is utilized in this research to study the flexural response of all beams. The flexural test is conducted using the Universal Testing Machine (UTM) available at the American University of Sharjah (AUS) laboratory, refer to Figure 8b. Hydraulic jacks are used to apply the load directly on the spreader beam. The role of the spreader beam is to divide the load equally on two points of 400 mm apart. The 400 mm distance is the constant maximum moment region. Strain guages are installed on the concrete beams and on the reinforcing bars to record the strians throughout the test. LVDT is installed below the beam to measure deflection. One LVDT is fixed under the beam at the center of the span. Crack transducers are utilized to measure the crack width during the tests, see Figure 9. All beams are cast at the same time from the same concrete mix and the test is conducted under normal conditions (23 ± 3^o C and 50 ± 10 % relative humidity).

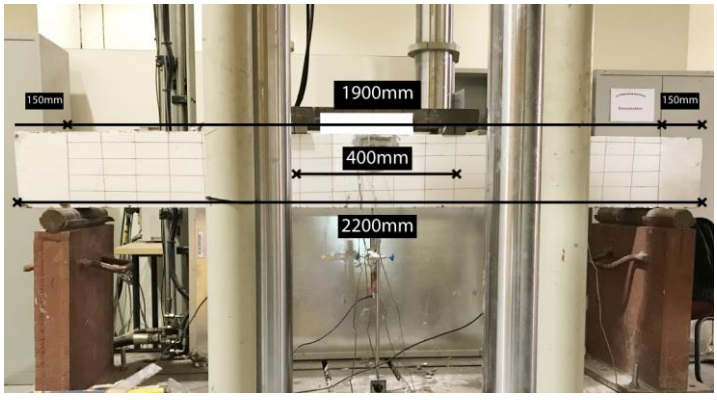

(a)

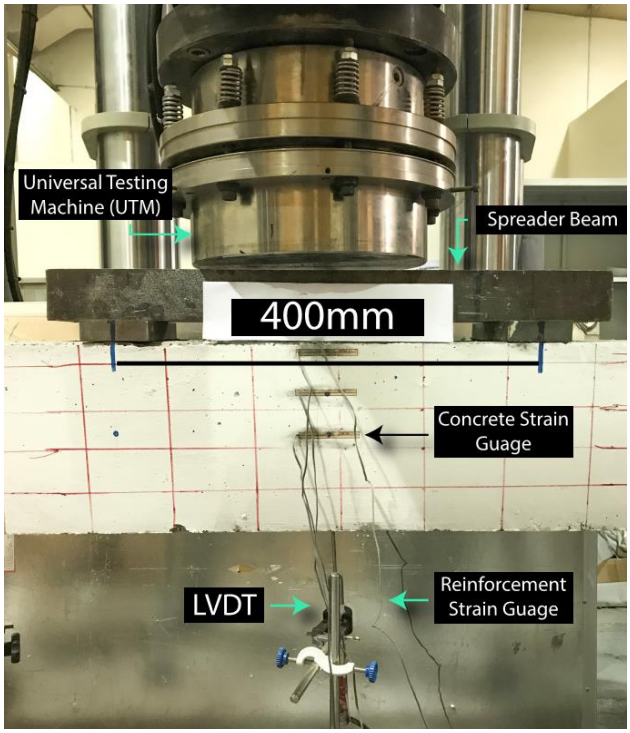

(b)

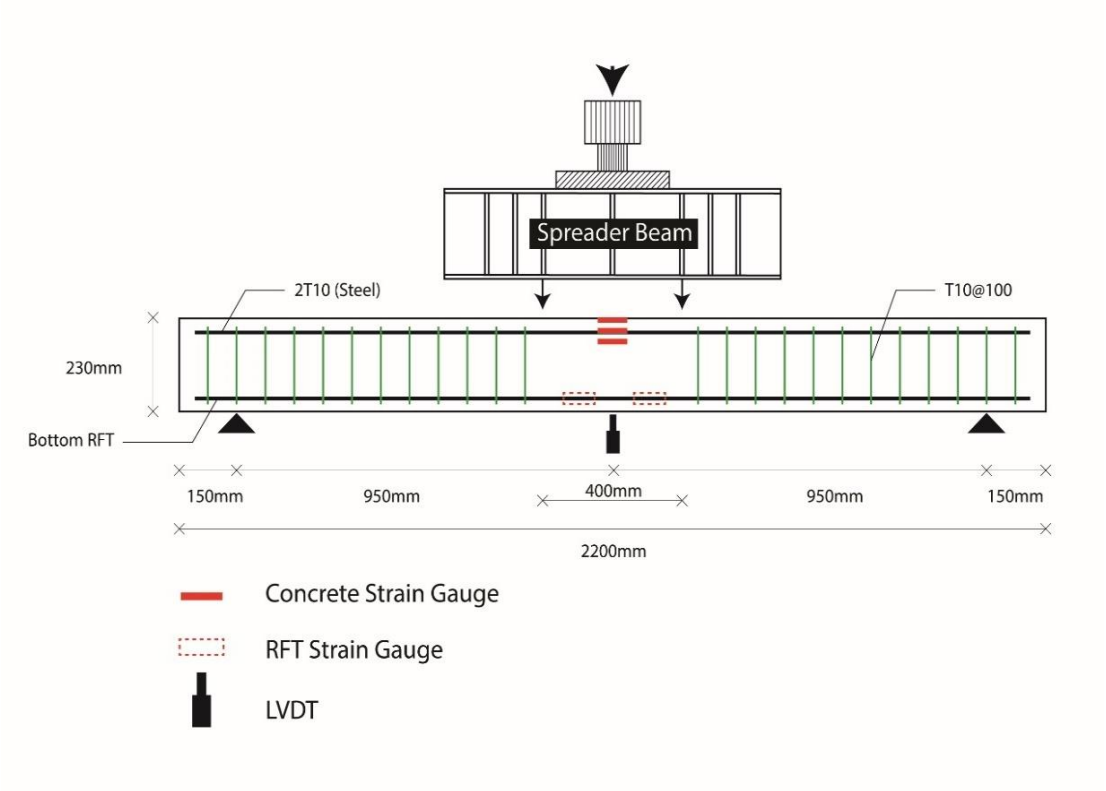

(c)

Figure 8: a) Beam's Elevation, b) Beam's testing Setup, c) Schematic Testing Setup

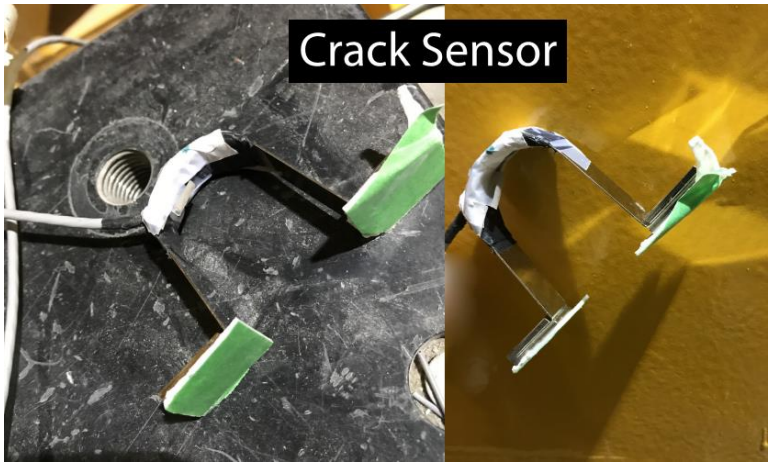

Figure 9: Crack Transducer

3.4 Testing Method

One of the main aims of this research is to determine the bond dependent factor of BFRP bars when used as flexural reinforcement in concrete beams. The test determines how the surface of the bar affects the bond with concrete.

The following points summarize the steps that are followed to evaluate the bond-dependent coefficient (k_b):

1. The load is applied until the first flexural crack appears. Then, the load is held constant to measure the initial crack width.
2. The load is resumed until the second flexural crack appears and the same procedure is repeated.
3. Load vs deflection is recorded
4. Strain in the reinforcement is recorded throughout the test
5. Strain in the concrete is recorded from the strain gauges attached at the top of the concrete beam
6. The load is kept until the crack width is more than 1mm and the beam fails.
7. The values of k_b are calculated at 33% of the maximum moment (M_n), at 67% of the maximum moment (M_n) and at crack width value equals to 0.7 mm.

Chapter 4: Design Philosophy

In this chapter, the theoretical equations suggested by the ACI 440.1R-15 code are presented, which then are used to compare with the experimental results obtained from the current study. The code equations include predicting the theoretical flexural capacities, calculating the deflection at midspan, and the evaluation of the bond-dependent coefficient (k_b).

4.1 The Flexural Capacity

The ACI 440.1R-15 code permits two modes of flexural failures when designing concrete beams reinforced with FRP bars [1]. The first failure mode is similar to the flexural failure that suggested by the ACI 318 code for steel reinforced beams, which the tension-controlled failure mode. FRP bars experience a sudden failure (FRP Rupture) since they do not have a defined yielding point. On the other hand, the second failure mode is concrete crushing, yet the concrete is considered as a brittle material, still the FRP bars show more plastic behavior than FRP rupture. Both failures are dependent on FRP reinforcement ratio. In order for the beam to be tension-controlled, the reinforcement ratio must be lower than the balanced reinforcement ratio ($\rho_f < \rho_{fb}$). On the contrary, to achieve a compression failure by concrete crushing, the reinforcement ratio of the beam should be greater than the balanced reinforcement ratio ($\rho_f > \rho_{fb}$). In this research, all beams that are reinforced with FRP bars are designed to fail in concrete crushing ($\rho_f > \rho_{fb}$).

Accordingly, the ACI 440.1R-15 imposes the use of reduction factor 0.65 for flexural members that are over reinforced in order to fail in concrete crushing. ACI 440.1R-15 enforces a reduction factor of 0.55 for beam that are designed to fail by FRP rupture. Concrete crushing exhibits more ductile behavior than FRP rupture. Beams that do not fail in either one of the two failure modes are considered to be in a transition zone [1].

Most likely, the flexural member that reinforced with FRP bars do not fail in concrete crushing as predicted. Generally, the reason for that is the variation in section geometry and material properties. Therefore, due to the mentioned reasons and factors, the ACI 440.1R-15 recommends using high strength concrete in order to utilize high strength of the FRP bars.

Moment capacity computations for the beam cross sections are done based on following assumptions (ACI440.1R-15):

1. A maximum usable compressive strain of concrete is 0.003.
2. Linear elastic behavior of the FRP reinforcing bars.
3. The FRP bars and concrete are bonded perfectly.
4. Plane section remains plane. The strain in the concrete and the FRP bars is proportional to the distance from the neutral axis.

The BFRP balanced reinforcement ratio can be defined as the amount of reinforcement needed to initiate tensile rupture of the reinforcement at the same time as concrete crushing.

$$\rho_{fb} = 0.85\beta_1 \frac{f'_C}{f_u} \left(\frac{E_f \varepsilon_c}{E_f \varepsilon_c + f_u}\right) \quad (1)$$

Where:

f'_c: Concrete compressive strength (MPa)

f_u : Design tensile strength of FRP (MPa)

ε_c: Ultimate concrete compressive strain

E_f: Elastic modulus of FRP bar (MPa)

β_1: refers to the ratio of the depth of the Whitney block to the depth of the neutral axis.

Table 7 shows typical values of the balanced reinforcement ratio for steel and different FRP bars for concrete compressive strength of *f'c* = 35 MPa as per ACI440.1R-15. In addition, the table clarifies that the FRP balanced reinforcement ratio (ρ_{fb}) is lower than the steel balanced reinforcement ratio (ρ_b). In order to design a beam in a way that is controlled by concrete crushing not FRP rupture, the beam shall be considered over-reinforced [1].

Table 7: Typical values for balanced reinforcement ratios as per ACI440.1R-15 [1]

Bar type	Yield strength f_y or tensile strength f_{fu}, ksi (MPa)	Modulus of elasticity, ksi (GPa)	ρ_b or ρ_{fb}
Steel	60 (414)	29,000 (200)	0.0335
GFRP	80 (552)	6000 (41.4)	0.0078
AFRP	170 (1172)	12,000 (82.7)	0.0035
CFRP	300 (2070)	22,000 (152)	0.0020

Equation (2) shows how the reinforcement ratio of a beam cross-section is calculated:

$$\rho_f = \frac{A_f}{bd} \tag{2}$$

where:

A_f: The total area of the FRP reinforcement used in the section (mm^2)

b: Width of the beam (mm)

d: Effective depth (mm) can be calculated as follows:

d= h − clear concrete cover − stirrups diameter − flexural bar diameter/2 (3)

When the reinforcement ratio of the beam (ρ_f) is greater than the balanced reinforcement ratio (ρ_{fb}) ($\rho_f > \rho_{fb}$), concrete crushing is controlling failure mode and the compression stress distribution of the concrete can be represented by the Whitney block, as illustrated in *Figure 10*. Equation (4) shows that the reinforcement ratio is utilized in calculating the nominal moment capacity of a section.

$$M_n = \rho_f f_f \left(1 - 0.59 \frac{\rho_f f_f}{f_c'}\right) bd^2 \tag{4}$$

Where f_f is the FRP stress at failure defined as follows:

$$f_f = \left(\sqrt{\frac{(E_f \varepsilon_c)^2}{4} + \frac{0.85\beta_1 f_C'}{\rho_f} E_f \varepsilon_c} - 0.5 E_f \varepsilon_c\right) \leq f_u \tag{5}$$

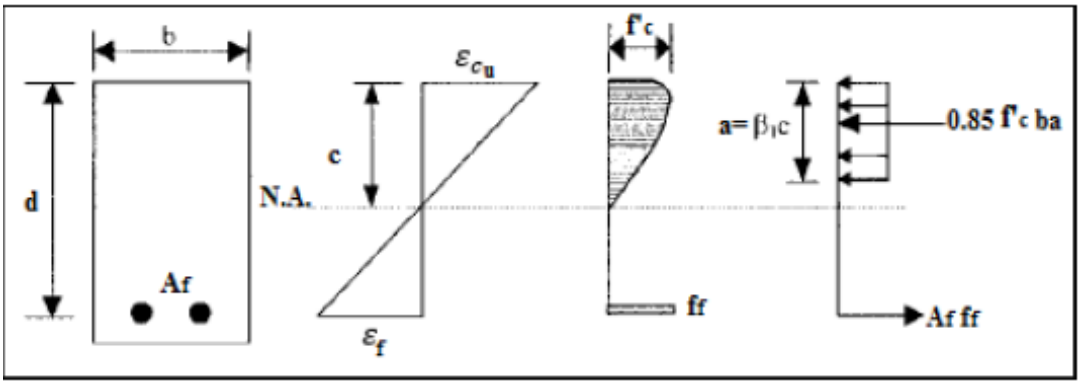

Figure 10: FRP Beam stress-strain diagram (Whitney block)

The ultimate applied moment should satisfy the following equations

$$M_n = A_f f_f (d - \frac{a}{2}) \tag{6}$$

$$a = \frac{A_f f_f}{0.85 f'_c b} \tag{7}$$

$$M_u \leq \varphi M_n \tag{8}$$

The reduction factor (φ) can be calculated as shown below:

$$\varphi = \begin{cases} 0.55 \; for \; (\rho_f \leq \rho_{fb}) \\ 0.3 + 0.25 \frac{\rho_f}{\rho_{fb}} for \; (\rho_{fb} < \rho_f < 1.4\rho_{fb} \\ 0.65 \; for \; (\rho_f \geq 1.4\rho_{fb}) \end{cases} \tag{9}$$

4.2 FRP Concrete Beam Deflection

The deflection of the FRP concrete beam can be calculated based on ACI 440-1R-15 code [1], using the following equations:

$$\Delta_i = \frac{Pa}{24 E_c (I_e)} (3l^2 - 4a^2) \tag{10}$$

$$I_e = (\frac{M_{cr}}{M_{Applied}})^2 \beta_d I_g \; + \left[1 - (\frac{M_{cr}}{M_{Applied}})^3\right] I_{cr} \leq I_g \tag{11}$$

$$\beta_d = \frac{1}{5}\left(\frac{\rho_f}{\rho_{fb}}\right) \leq 1 \tag{12}$$

Where:

$M_{applied}$= Moment due to applied load (N.mm)

l= Span length (mm)

E_c= Concrete modulus of elasticity (MPa)

I_e= Effective moment of inertia (mm^4)

$$I_{cr} = \frac{bd^3}{3} k^3 + \; n_f A_f d^2 (1 - k)^2 \tag{13}$$

$$f_r = 0.62\sqrt{f'_c} \tag{14}$$

$$M_{cr} = \frac{2 f_r I_g}{h} \tag{15}$$

$$I_g \; = \frac{bh^3}{12} \tag{16}$$

I_{cr}= Moment of inertia of cracked section (mm^4)

β_d= Reduction factor related to the reduced tension stiffening of FRP beams

I_g= Gross moment of inertia for the section (mm^4)

ρ_f= FRP reinforcement ratio

ρ_{fb}= FRP balanced reinforcement ratio

f_r= Modulus of rupture (MPa)

h= Depth of the beam (mm)

b= Width of the beam (mm)

4.3 Bond-dependent Coefficient (k_b)

The bond-dependent coefficient (k_b) is verifiably derived from the tested specimen where many factors are considered such as beam's section and dimension, FRP bar properties and the strain in the FRP bars that is carefully measured. After the initial cracking has occurred, the crack widths are measured using the crack sensor, then the bond dependent coefficient for the FRP bars is calculated equation (8-9) in ACI440.1R-15 [1].

$$w = 2\frac{f_f}{E_f}\beta \times k_b \times \sqrt{d_c^2 + \left(\frac{s}{2}\right)^2} \quad (17)$$

The k_b factor is calculated at three stages: a) at 33% of the maximum moment capacity of the section (M_n) b) at 67% of the maximum moment capacity of the section (M_n) c) at crack width value (w) equals to 0.7. The mean of the three values is considered in calculating the effective k_b of the reinforcement bars.

w: Maximum crack width (mm)

E_f : Modulus of elasticity of FRP bar (MPa)

f_f: Stress in FRP reinforcement in tension (MPa)

k_b: Bond-dependent coefficient

β: Ratio of distance from neutral axis to extreme tension fiber to distance from neutral axis to center of tensile reinforcement

d_c: Thickness of concrete cover measured from extreme tension fiber to center of bar (mm)

s: Longitudinal FRP bar spacing (mm)

Chapter 5: Experimental Results

In this chapter, results of experimental tests for concrete beam specimens reinforced with the newly revealed BFRP bars are presented. Load versus mid-span deflection curves, along with modes of failure and strains are presented as well. Discussion and analysis of results, considering four different bar sizes of BFRP and two different concrete compressive strengths (normal and high) are presented in the next chapter.

5.1 Load versus Mid-Span Deflection Relationships

Figures 11 and 12 present the load versus mid-span deflection for the tested beams cast with concrete compressive strengths of 30 MPa and 60 MPa, respectively. Figure 11a illustrates the graphs of the BFRP-reinforced concrete beams. On the other hand, the load versus mid-span deflection curves of the CFRP-reinforced and steel-reinforced concrete beams are shown in Figure 11b.

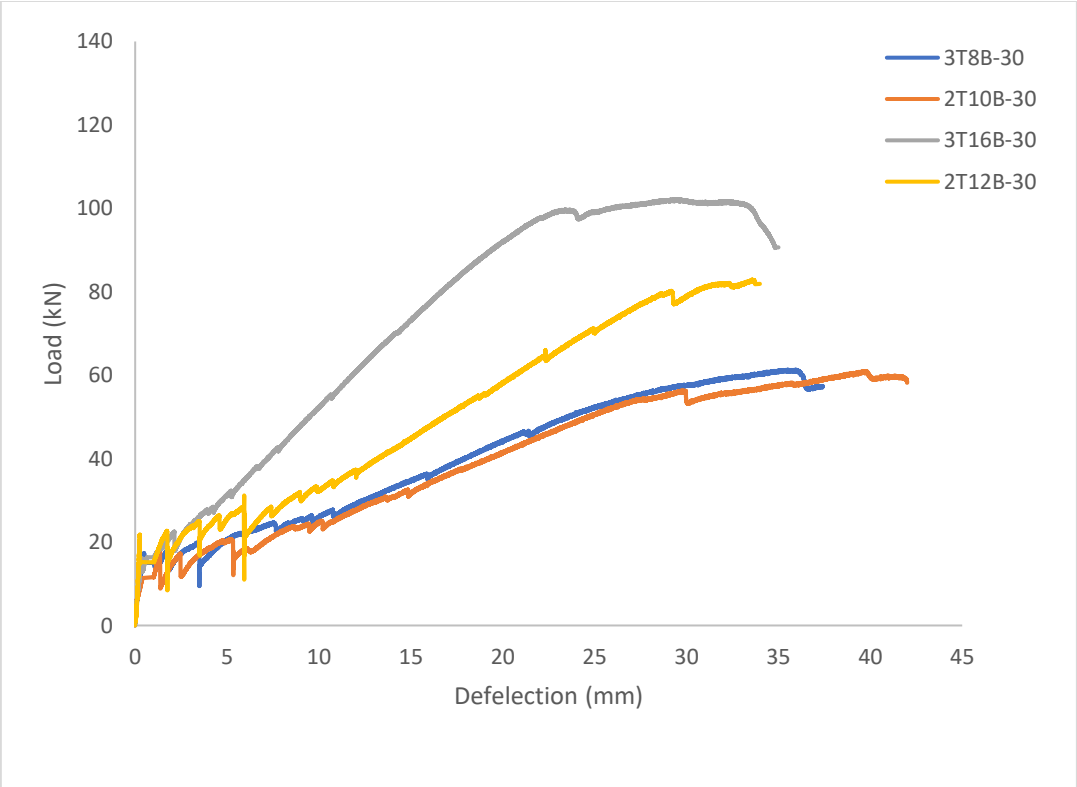

(a)

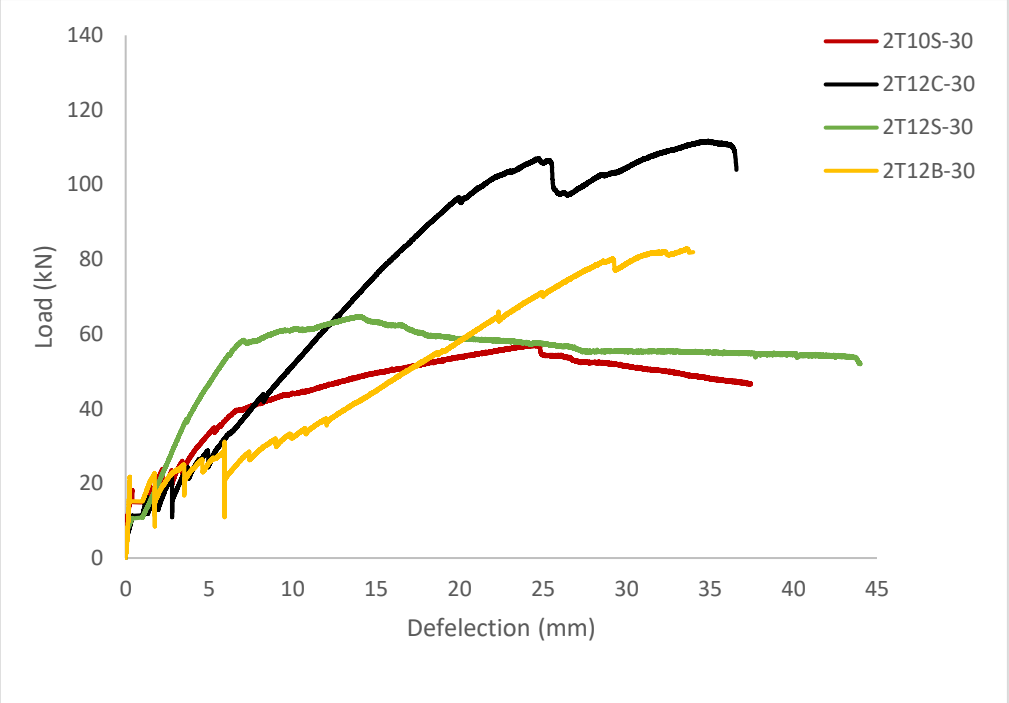

(b)

Figure 11: Experimental load vs mid-span deflection for beams cast with f'_c=30 MPa (a) beams reinforced with BFRP bars, (b) beams reinforced with CFRP and Steel bars

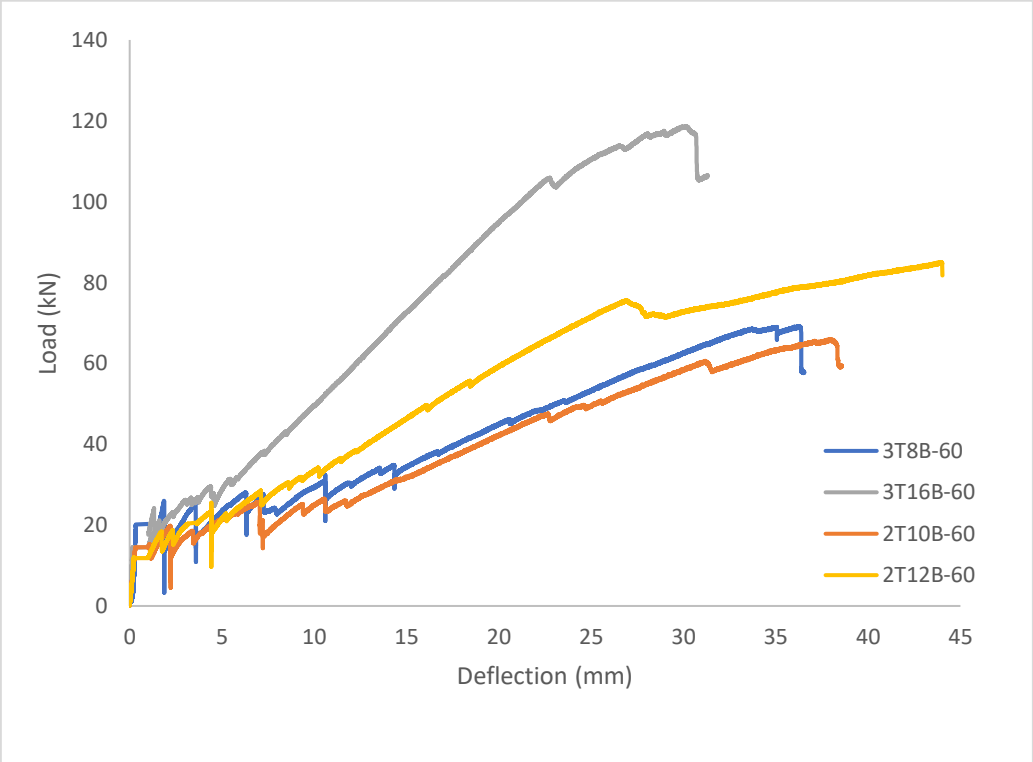

(a)

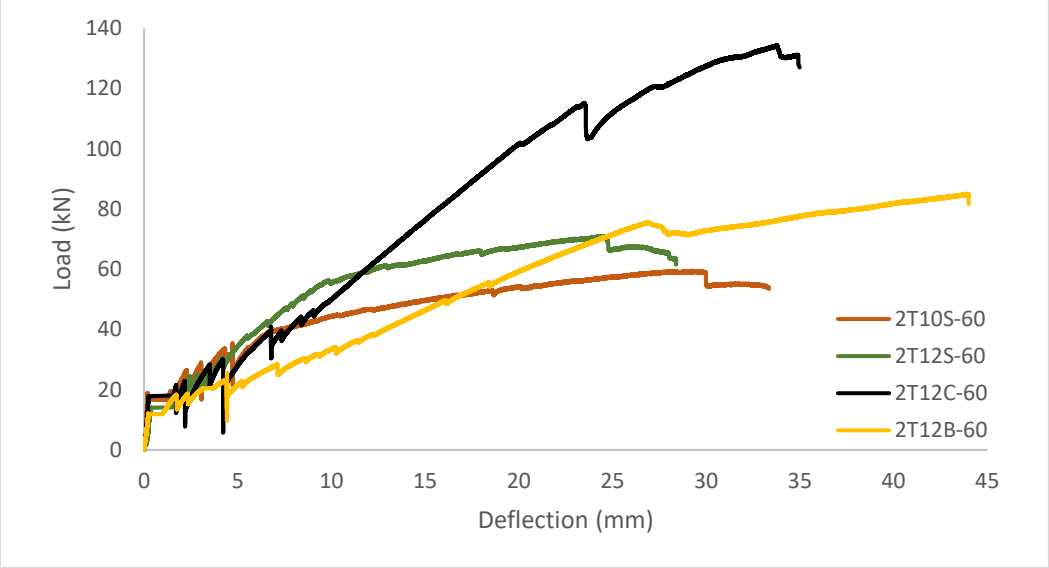

(b)

Figure 12: Experimental load vs mid-span deflection for beams cast with f'_c=60 MPa (a) beams reinforced with BFRP bars, (b) beams reinforced with CFRP and Steel bars

Tables 8 and 9 show the maximum loads, moment capacities, maximum deflections and first cracking loads of beams with compressive strength value of 30 MPa and 60 MPa, respectively. Moreover, both tables describe the failure modes of each beam depending on the reinforcement type.

Table 8: Summary of flexural test results f'_c =30 MPa

Beam	Max Load (kN)	Max Moment capacity (kN.m)	Max. Mid-span deflection (mm)	First cracking Load (kN)	Failure mode
3T8B-30	61.3	23	37.4	18	Concrete crushing
2T10B-30	61	22.9	42	14	Concrete crushing
2T12B-30	83	31.1	34	22	Concrete crushing
3T16B-30	102	38.3	35	16	Concrete crushing
2T12C-30	111.7	41.9	36.5	16	Concrete crushing
2T10S-30	57.2	21.4	37.5	18	Steel Yielding (Tension-Controlled)
2T12S-30	64.8	24.3	44	17	Steel Yielding (Tension-Controlled)

Table 9: Summary of flexural test results f'_c =60 MPa

Beam	Max Load (kN)	Max Moment capacity (kN.m)	Max. Mid-span deflection (mm)	First cracking Load (kN)	Failure mode
3T8B-60	69.2	26	36.5	26	Concrete crushing
2T10B-60	65.9	24.7	38.6	15	Concrete crushing
2T12B-60	85	31.9	44	23	Concrete crushing
3T16B-60	118.6	44.5	31.3	24	Concrete crushing
2T12C-60	134.3	50.4	35	21	Concrete crushing
2T10S-60	59.5	22.3	33.4	19	Steel Yielding (Tension-Controlled)
2T12S-60	71	26.6	28.4	20	Steel Yielding (Tension-Controlled)

5.2 Crack Behavior

In this section, the load versus crack width and the cracking patterns are presented for all the tested beams. All figures present the cracking behavior of beams cast with different concrete compressive strengths of 30 MPa and 60 MPa. In addition, the load of the first 8 cracks of all the tested beams are displayed. The values of the theoretical cracking moment versus the experimental cracking moments are displayed as well.

5.2.1 Load versus crack width relationship. Figure 13 shows the load versus crack width relationship of beams cast with concrete compressive strength of 30 MPa. The relationships for beams reinforced with different diameters of Basalt FRP bars are displayed in Figure 13a, and for beams reinforced with Carbon FRP and steel bars are shown in Figure 13b. Furthermore, these figures indicate the average service loads of all beams and the crack width limit of 0.7 mm specified by ACI code. The graph starts from the value of the first crack. The graphs show the linear relationship between the load and the crack width. Similar results are presented in Figure 14 for beams cast with high compressive strength ($f'c$ = 60 MPa).

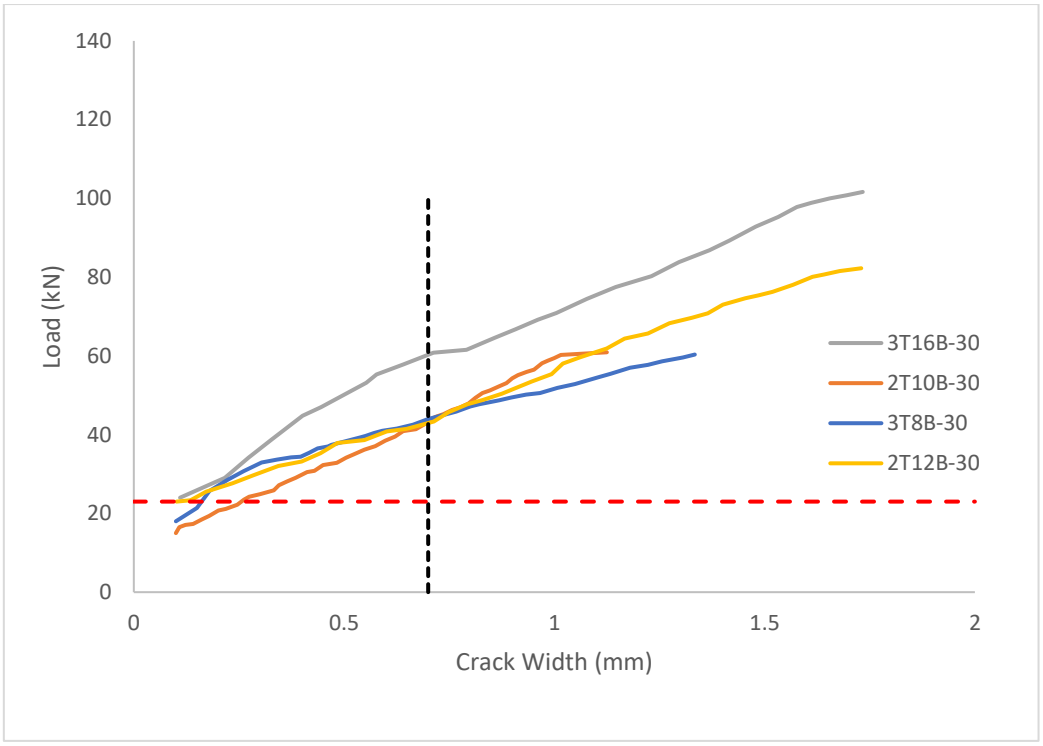

(a)

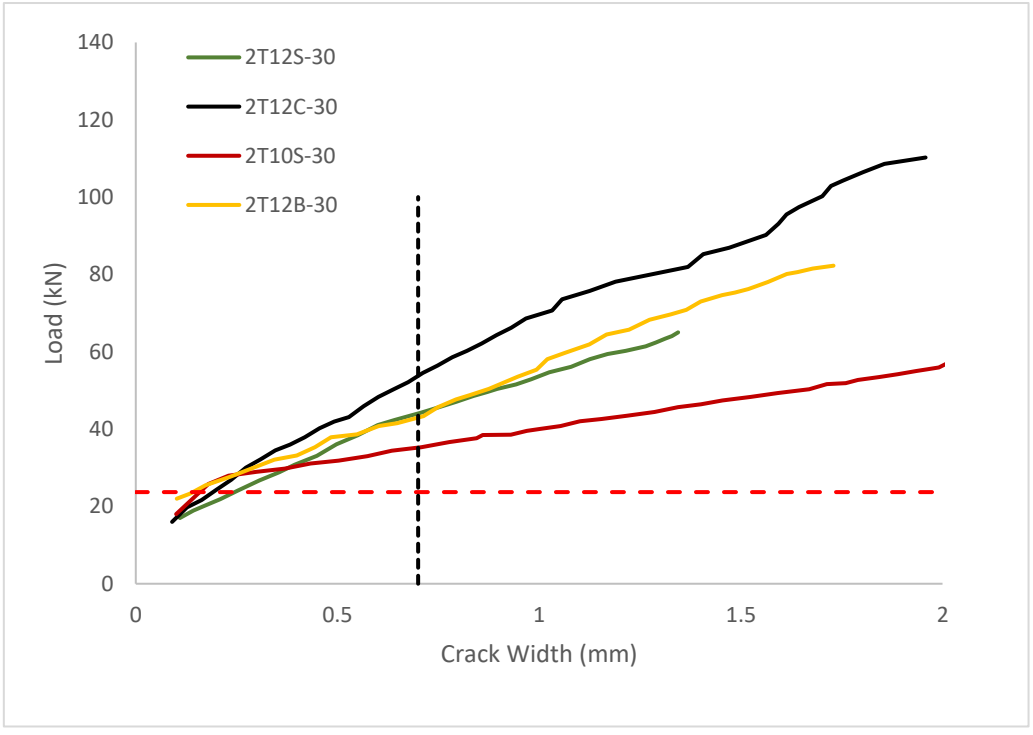

(b)

ACI limit Average Service Load

Figure 13: Moment vs crack width for beams cast with f'_c=30 MPa (a) beams reinforced with BFRP bars, (b) beams reinforced with CFRP and Steel bars

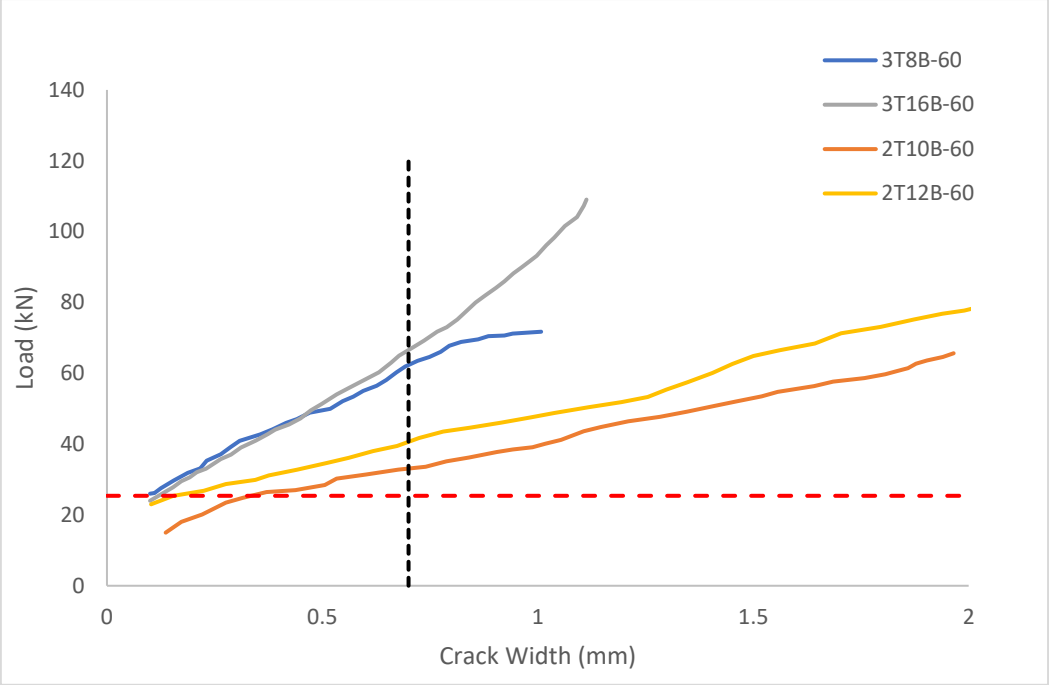

(a)

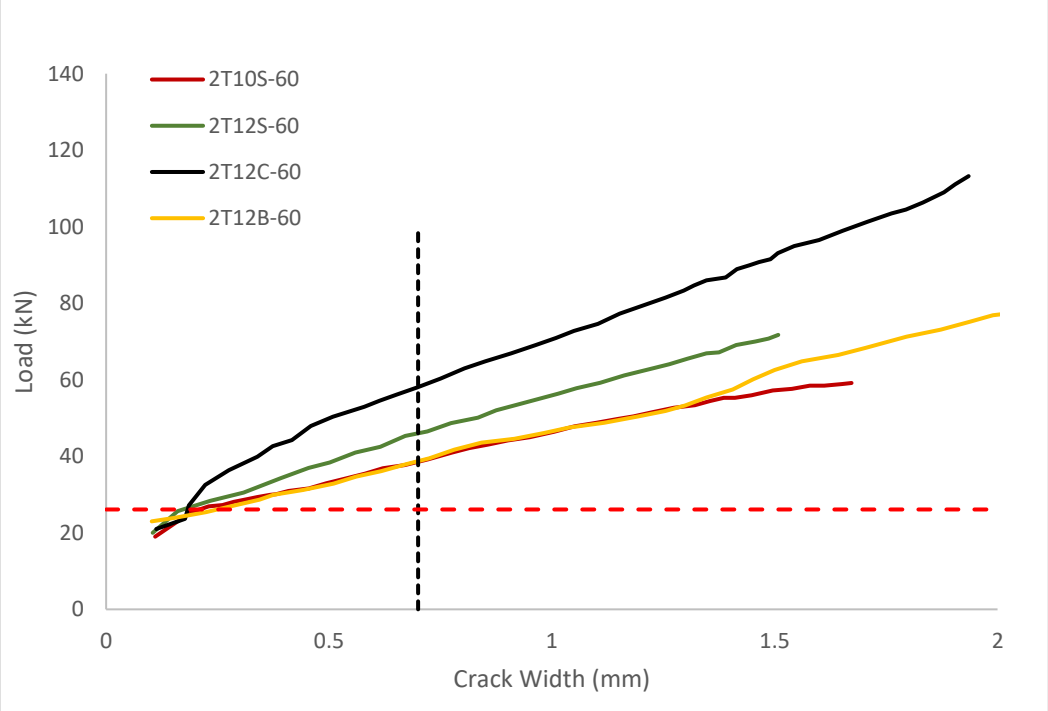

(b)

ACI limit Average Service Load

Figure 14: Moment vs crack width for beams cast with f'_c=60 MPa (a) beams reinforced with BFRP bars, (b) beams reinforced with CFRP and Steel bars

5.2.2 Crack pattern. The crack patterns of all the tested beams are monitored during the flexural test and throughout the different loading stages. Figure 15 shows the crack patterns for the tested beams at the service loading stage. In addition, Figure 16 displays the crack patterns at ultimate loading. Moreover, the loads at which each crack developed are recorded and listed in Tables 10 and 11. Table 10, displays the initiation load of the first 8 cracks in the beams cast with concrete compressive strength = 30 MPa. On the other hand, Table 11 shows the loads at which the first 8 cracks have occurred for the beams cast with 60 MPa concrete compressive strength. All the tested beams are assembled in groups and compared to each other based on the research objectives mentioned before and are discussed in the next chapter.

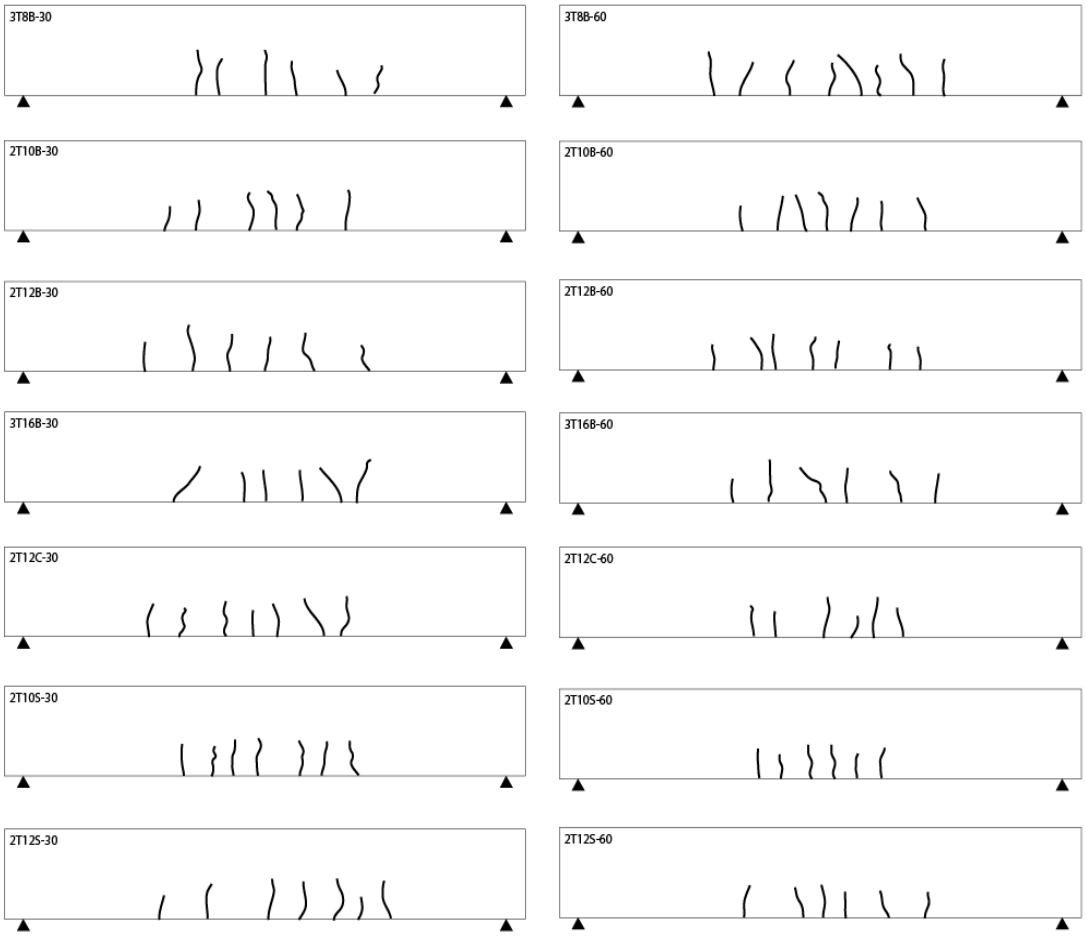

Figure 15: Crack pattern at service load stage (a) beams cast with f'_c=30 MPa, (b) beams cast with f'_c = 60 MPa

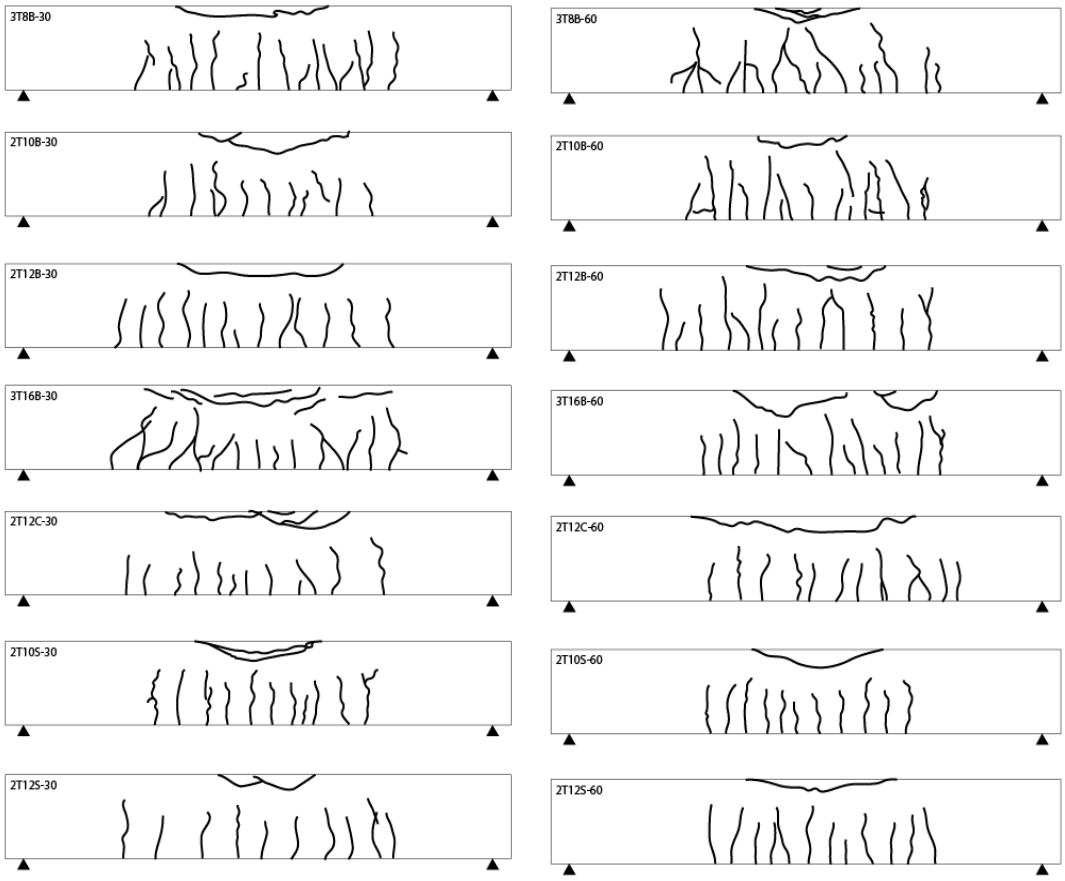

(a) (b)

Figure 16: Crack pattern at ultimate load stage (a) beams cast with f'_c=30 MPa, (b) beams cast with f'_c = 60 MPa

Table 10: Cracking Loads, f'_c =30 MPa

# No	Beam	Crack number							
		1	2	3	4	5	6	7	8
		Load for each crack (kN)							
1	3T8B-30	18	19	20	22	23	24	25	26
2	2T10B-30	16	17	18	20	21	23	24	24
4	2T12-B-30	22	23	24	25	25	26	28	29
3	3T16B-30	16	19	22	23	27	29	30	36
5	2T12C-30	16	17	20	28	25	29	33	44
6	2T10S-30	18	19	21	23	25	36	38	42
7	2T12S-30	17	21	24	28	30	38	40	45

Table 11: Cracking Loads, f'_c =60 MPa

# No	Beam	Crack number							
		1	2	3	4	5	6	7	8
		Load for each crack (kN)							
1	3T8B-60	26	27	28	29	29	30	31	32
2	2T10B-60	20	20	21	22	23	25	27	28
3	2T12-B-60	23	24	25	27	28	29	32	35
4	3T16B-60	24	25	26	26	27	28	29	30
5	2T12C-60	21	22	24	25	35	37	41	48
6	2T10S-60	19	21	25	28	33	35	36	37
7	2T12S-60	20	25	30	34	36	39	49	58

Tables 12 and 13 show a comparison between the experimental cracking moment and the predicted (theoretical) cracking moment for beams cast with f'_c=30 MPa and f'_c=60 MPa, respectively. The modulus of rupture and the cracking moments are calculated as per equations 14 and 15.

Table 12: Experimental vs theoretical cracking moment, beams cast with f'_c=30 MPa

Beam	Load of First crack (kN)	Experimental M_{cr} (kN.m)	Predicted M_{cr} (kN.m)	Exp. M_{cr}/Pred. M_{cr}
3T8B-30	18	6.75	6.07	1.11
2T10B-30	16	6	6.07	0.99
2T12B-30	22	8.25	6.07	1.36
3T16B-30	16	6	6.07	0.99
2T12C-30	16	6	6.07	0.99
2T10S-30	18	6.75	6.07	1.11
2T12S-30	17	6.375	6.07	1.05

Table 13: Experimental vs theoretical cracking moment, beams cast with f'_c=60 MPa

Beam	Load of First Crack (kN)	Experimental M_{cr} (kN.m)	Predicted M_{cr} (kN.m)	Exp. M_{cr}/Pred. M_{cr}
3T8B-60	26	9.75	7.39	1.32
2T10B-60	20	7.5	7.39	1.01
2T12B-60	23	8.625	7.39	1.17
3T16B-60	24	9	7.39	1.22
2T12C-60	21	7.875	7.39	1.07
2T10S-60	19	7.125	7.39	0.96
2T12S-60	20	7.5	7.39	1.01

5.3 Load versus Strain Relationships

The strain values of the longitudinal reinforcement and concrete are captured using strain gauges installed at mid-span of the reinforcement and the concrete section. The strain values for the longitudinal reinforcement and their corresponding loads for all the tested beams are shown in Figures 17 and 18. In Addition, the ultimate strain values at the top fibers of the concrete beams and in the longitudinal reinforcement are recorded and summarized in Tables 14 and 15.

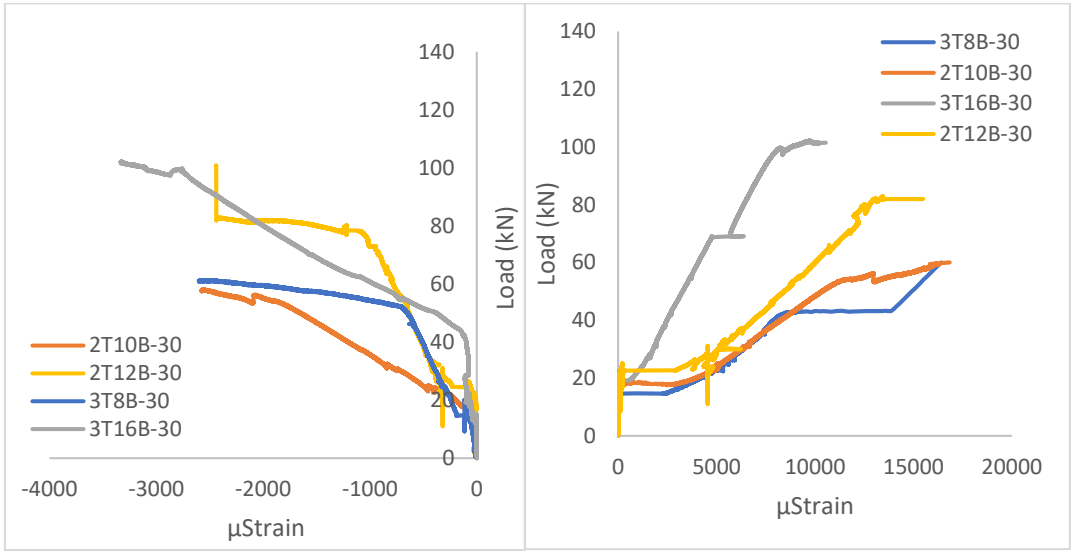

(a)

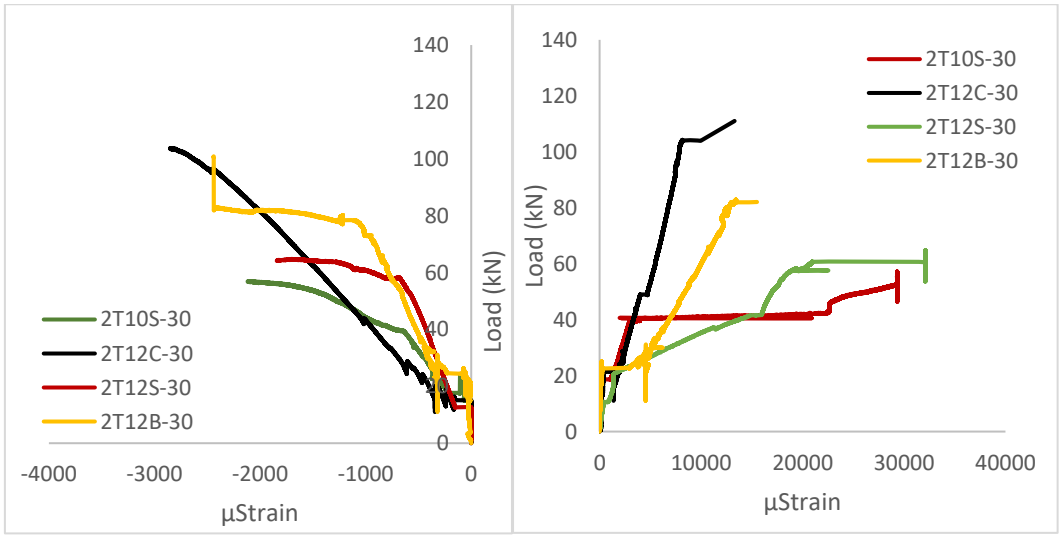

(b)

Figure 17: Load vs Strain values of concrete and reinforcement, f'_c =30 MPa

(a) beams reinforced with BFRP bars, (b) beams reinforced with CFRP and Steel bars

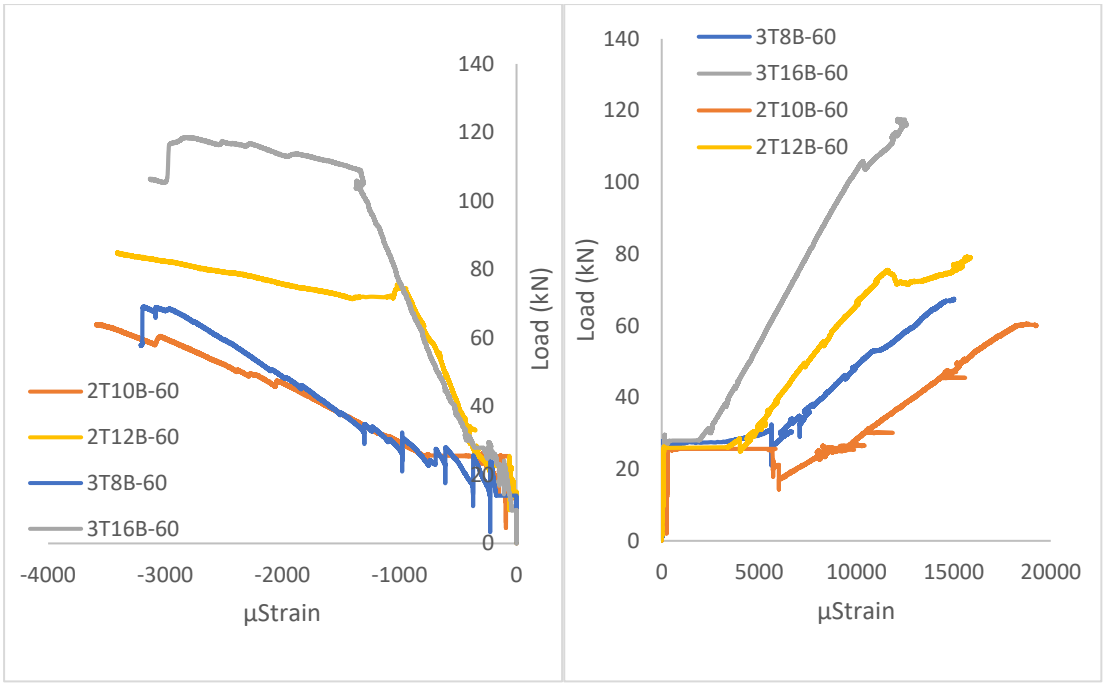

(a)

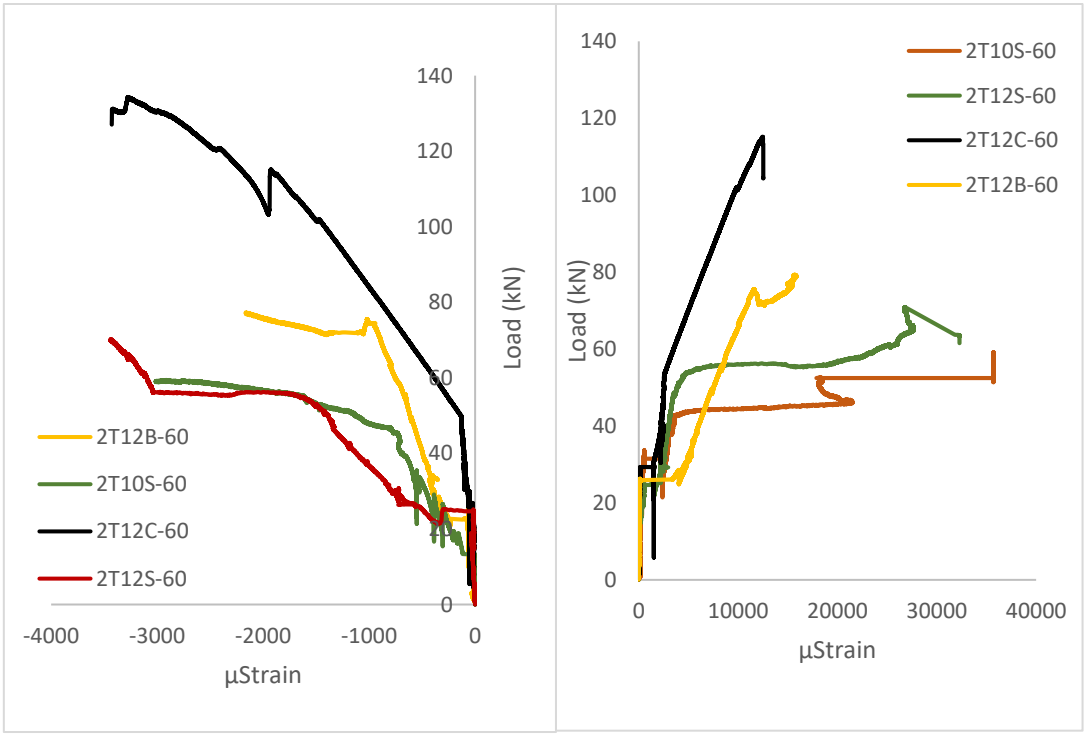

(b)

Figure 18: Load vs Strain values of concrete and reinforcement, f'_c =60 MPa beams reinforced with BFRP bars, (b) beams reinforced with CFRP and Steel bars

Table 14: Load vs concrete and reinforcement strain, f'_c =30 MPa

# No	Beam	Load (kN)	Longitudinal reinforcement strain	Concrete Strain
1	3T8B-30	61.3	0.0164	0.0026
2	2T10B-30	61	0.0169	0.0028
3	2T12B-30	83	0.0155	0.0028
4	3T16B-30	102	0.0106	0.0033
5	2T12C-30	111.7	0.0133	0.0028
6	2T10S-30	57.2	0.029	0.0022
7	2T12S-30	64.8	0.032	0.0019

Table 15: Load vs concrete and reinforcement Strain, f'_c =60 MPa

# No	Beam	Load (kN)	Longitudinal reinforcement strain	Concrete Strain
1	3T8B-60	69.2	0.0163	0.0032
2	2T10B-60	65.9	0.019	0.0039
3	2T12B-60	85	0.0159	0.0034
4	3T16B-60	118.6	0.0126	0.0031
5	2T12C-60	134.3	0.0125	0.0034
6	2T10S-60	59.5	0.0357	0.003
7	2T12S-60	71	0.0323	0.0034

Chapter 6: Results Discussion

In this chapter, the results of the experimental program for all tested specimens are discussed. The discussion includes responses of load versus mid-span deflection, cracking behavior and mode of failure. The analysis and discussion of the results, including the effect of reinforcement ratio, reinforcement type and concrete compressive strength are presented as well.

6.1 Effect of Reinforcement Ratio (ρ)

Figure 19 shows the relationship between the moment capacity and the reinforcement ratio of the BFRP-reinforced beams. The figure demonstrates that increasing the reinforcement ratio leads to increasing the moment capacity; however, this behavior is not directly proportional, which proves the nominal capacity equation (4) in the ACI 440.1R-15. Furthermore, the graph shows that the increase followed similar trend of ACI 440 equation. For instance, the percentage increase in reinforcement ratio between beams 2T10B-30 and 2T12B-30 is 45% yielded a percentage increase in the moment capacity of 36%. In addition, the moment capacity has increased by 23% when the reinforcement ratio increases by 170% from 2T12B-30 to 3T16B-30. Similarly, the beams cast with higher concrete strength showed similar increasing trend as shown in Figure 19b. For example, after increasing the reinforcement ratio by 52% for beams 3T8B-60 and 2T12B-60 and 170% for beams 2T12B-60 and 3T16B-60, the moment capacity increased by 23% and 40%, respectively. Similar behavior was obtained by Abed et al. [20].

The values of the experimental cracking moment of the beams vary from 6 to 8.25 kN.m with an average value of 6.75 kN.m for the beam cast with 30 MPa concrete strength. The average cracking moment is approximately 23% of the average moment capacity of the beams. For the BFRP- reinforced beams that are cast with 60 MPa concrete strength, the average cracking moment values ranged between 7.5 and 9.75 kN.m with an average of 8.6 kN.m which has a percentage of 27% of the mean moment capacity value. Increasing the reinforcement ratio of the beams did not have a clear effect on increasing the cracking moment value. In fact, the reinforcing bars do not get engaged in carrying the load until the first crack in the concrete occurs. Theoretically,

as shown in ACI equations (14) and (15), the cracking moment is a function of the modulus of rupture which in turn is a function of the concrete compressive strength. The results obtained confirms the equations of predicting the cracking moment. Tables 12 and 13 display the experimental and the theoretical cracking moment values.

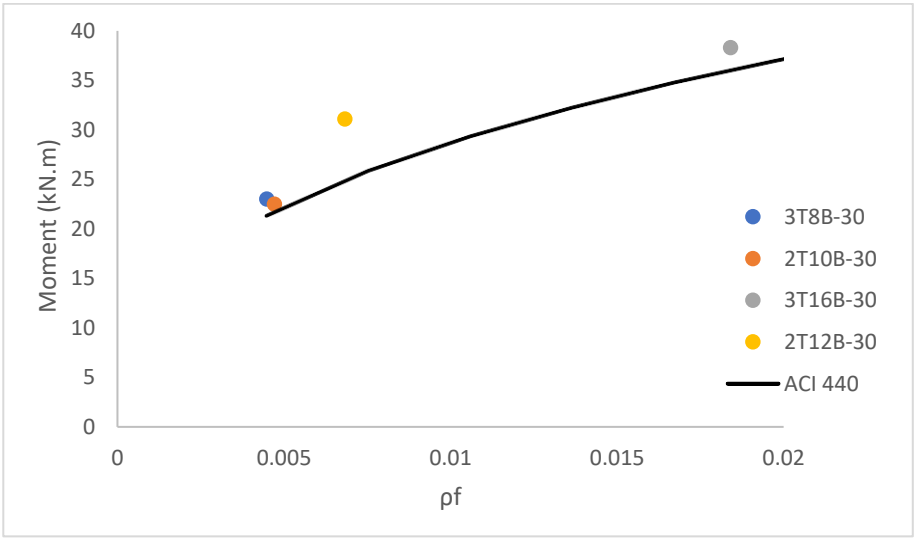

(a)

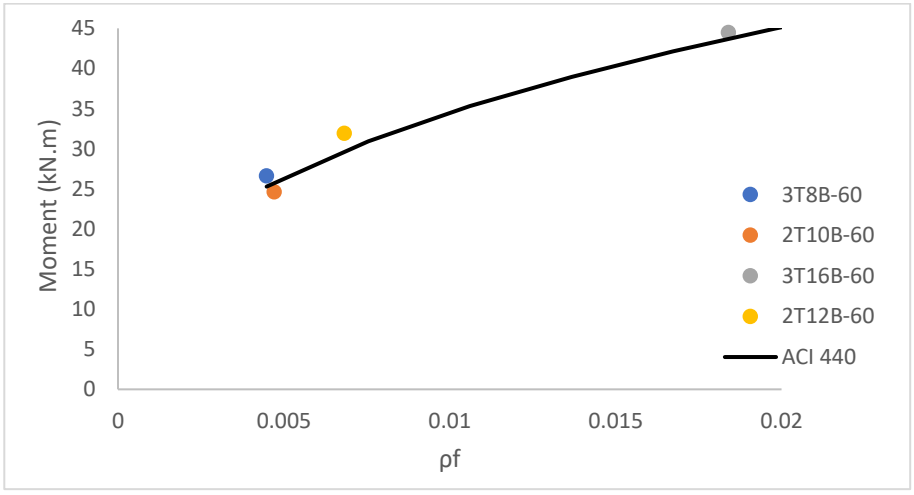

(b)

Figure 19: Ultimate moment vs reinforcement ratio for beams reinforced with BFRP bars, (a) beams cast with f'_c = 30 MPa, (b) beams cast with f'_c = 60 MPa

The cracking patterns at service load of all the tested beams are shown in Figure 15. The cracks initiated at the middle of the beam span in the constant moment region. The initiated cracks are vertical and perpendicular to the area of maximum tension. As

the load increases, more cracks are initiated which result in reducing the spacing between the cracks. The beams with higher reinforcement ratios experienced more tensile cracks than the beams with lower reinforcement ratios. The cracks markings of all the tested beams at ultimate loading stage are presented in Figure 16. The figure shows the cracks propagation at the pure moment region towards the compression zone where concrete crushing occurs. Figures 13a and 14a show the propagation of the width of the first crack with loads for the BFRP-reinforced beams that are cast with concrete strength of 30 MPa and 60 MPa, respectively. The figures clarify that the beams with higher number of bars experienced smaller crack widths at the same load level. The beams reinforced with 3T8 and 3T16 BFRP bars had lesser crack widths than the beams reinforced with 2T10 and 2T12 BFRP bars. This behavior approves equation (15) in the ACI440.1R-15 code of calculating the crack widths. Increasing the number of reinforcing bars in the beam decreases the spacing between that bars, thus reducing the crack widths. In addition, increasing the number of bars results in lower strain values in the bars which lead to smaller crack widths. On the other hand, increasing the reinforcement ratio has no significant impact on the crack widths value. This can be clearly observed in Figures 13a and 14a in the curves of the beams that are reinforced with 2T10 and 2T12 BFRP bars. Similar behavior was reported by Elgabbas et al. [25] and Elgabbas et al. [35].

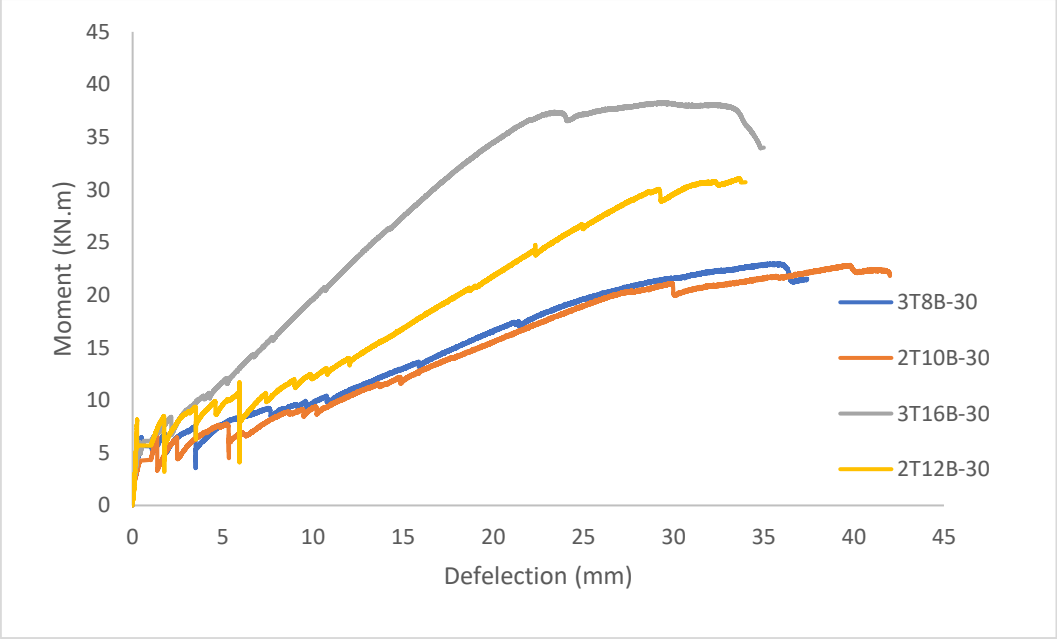

(a)

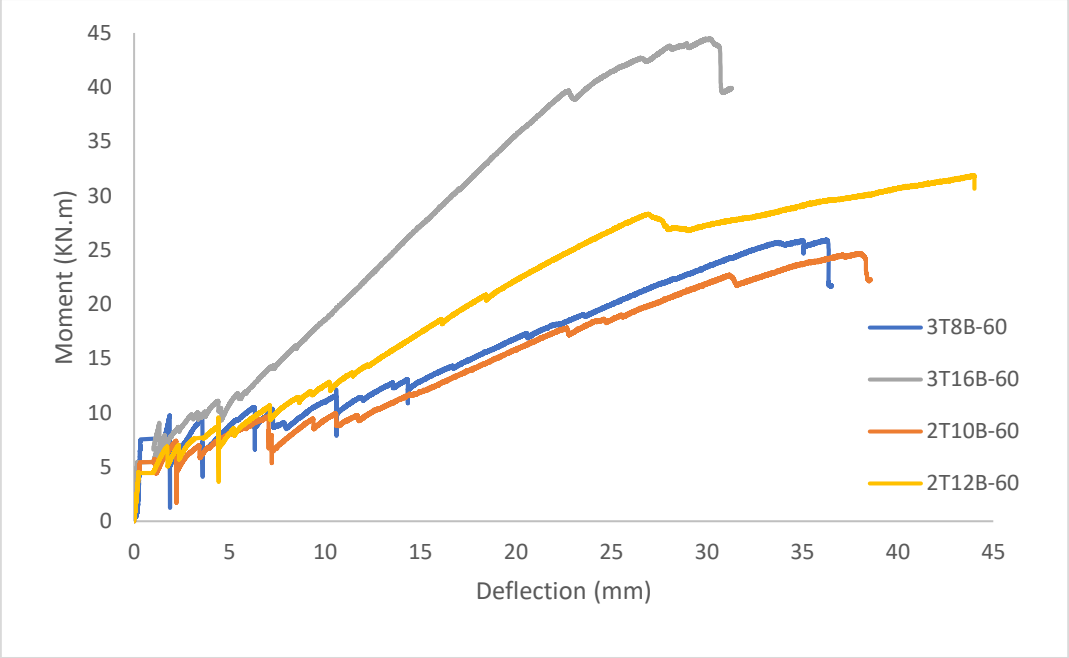

(b)

Figure 20: Moment vs Deflection for beams with BFRP bars, (a) beams cast with f'_c = 30 MPa, (b) beams cast with f'_c = 60 MPa

In addition, increasing the number of reinforcing bars, but keeping the same axial stiffness of the reinforcement, has negligible effect on the load carrying capacity of the beams. However, the beams with more reinforcing bars exhibited lower values of deflection. For example, as shown in Figure 11a, beam 2T10B-30 showed a higher deflection value of 42 mm compared to 37.4 mm for 3T8B-30 although both have a similar reinforcement axial stiffness value of 7.5 MN (EA = 7.5 MN). The reason is that in the beam reinforced with two bars, the bars engage in the load carrying capacity and exhibit higher strain values compared to the three bars where the strain is shared among the three bars. Similar behavior is obtained in the beam cast with 60 MPa concrete compressive strength; beam 2T10B-60 reached a deflection value of 38.6 mm which is slightly higher than a deflection value of 36.5 mm for 3T8B-60, as shown in Figure 12a.

The failure modes of the BFRP-reinforced beams are shown in Figures 21 and 22. All the BFRP-reinforced beam failed in concrete crushing. The beams were designed such that the maximum compressive stress in the concrete (at ε_{cu} = 0.003-0.004) is achieved prior reaching ultimate stress in the BFRP bars (f_{fu}). Tables 14 and

15 shows the strain values in the longitudinal reinforcement and the concrete of all the beams. The tables display that the concrete strain in BFRP-reinforced beams reached the crushing limit before the ultimate strain in the BFRP bars is reached. Increasing the concrete compressive strength value has slightly increased the ultimate strain of the concrete which contributed in delaying the failure and increasing the load-carrying capacity.

All the beams that are reinforced with BFRP bars showed similar behavior prior to cracking. Figure 20 illustrates the moment versus deflection curves of the BFRP-reinforced beams. After the occurrence of the first crack, the stiffnesses of the beams reduce and the reinforcement start getting involved in resisting the load. The BFRP bars exhibited a linear behavior until concrete crushing is achieved due to its elastic properties. Both beams 2T10B-30 and 3T8B-30 showed similar behavior and reached a maximum moment value of 23 kN.m because of the close axial stiffness (EA) value of 7.5 MN. Similarly, the beams 2T10B-60 and 3T8B-60 resisted moment values of 24.7 and 26.0 kN.m, respectively. As per the moment capacity equation (6) in the ACI440.1R-15, increasing the moment capacity can be achieved by increasing the reinforcement ratio in the beams. This can be clearly observed in the beams reinforced with 2T12 and 3T16 BFRP bars.

3T8B-30

2T10B-30

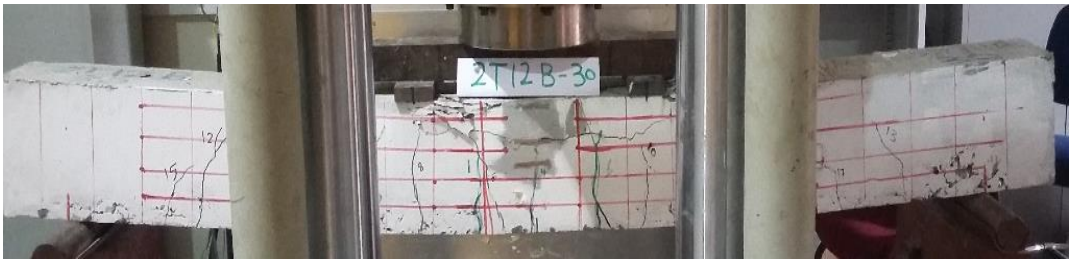

2T12B-30

3T16B-30

Figure 21: Failure modes of concrete beams reinforced with BFRP bars, beams cast with f'_c=30 MPa

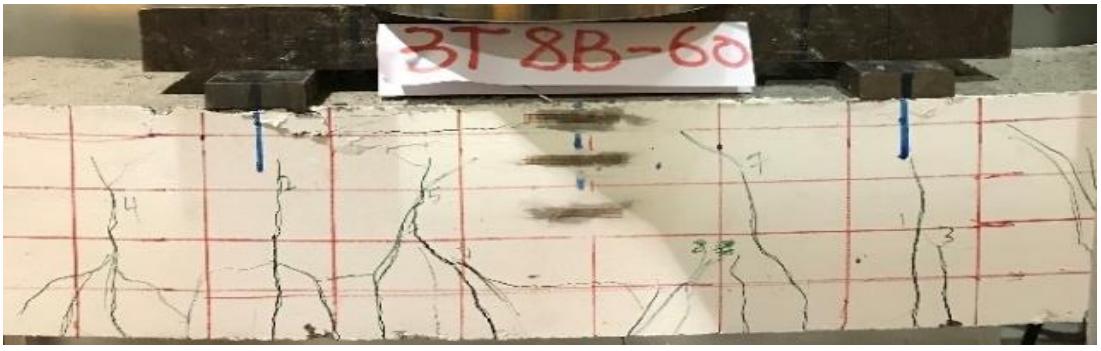

3T8B-60

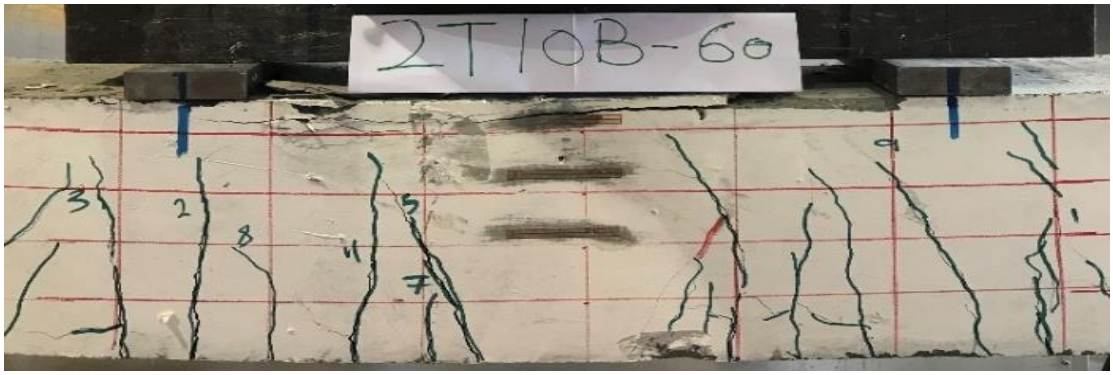

2T10B-60

2T12B-60

3T16B-60

Figure 22: Failure modes of concrete beams reinforced with BFRP bars, beams cast with f'_c=60 MPa.

6.2 Response of BFRP versus CFRP and steel RC beams

The response of the BFRP-reinforced beams is studied and compared to the beams that are longitudinally reinforced with CFRP and steel bars. The beams that are reinforced with FRP bars (BFRP and CFRP) achieved higher moment capacity than the beams reinforced with steel bars. The beams that have similar reinforcement ratios (2T12B, 2T12C and 2T12S) achieved different moment capacities due to the variance in the ultimate strength of the reinforcing bars. Figure 23 shows the moment versus deflection of beams reinforced with Basalt FRP, Carbon FRP and conventional steel bars and cast with concrete compressive strength of 30 and 60 MPa. In addition, Tables 8 and 9 summarize the maximum load and moment capacities attained in all the tested beams. With respect to the beams cast with 30 MPa concrete strength, beam 2T12C-30

reached a moment value of 41.9 kN.m which is 35% more than moment recorded by 2T12B-30 (31.1 kN.m) and 81.6% more than 2T12S-30 (24.3 kN.m). The Basalt and Carbon FRP beams showed different percentage increase when cast with 60 MPa concrete compressive strength. In this regard, the ultimate moment of CFRP Beam 2T12C-60 increased by 20.3%; whereas, the moment capacity of the BFRP Beam 2T12B-60 increased only by 4.0%. As indicated earlier, the increase in the ultimate capacity is attributed to the increase in concrete strain at ultimate, see Table 15. However, the large variation in the percentage increase between the two types of bars is mainly related to their Elastic Modulus values, refer to Table 2.

The flexural response of concrete beams reinforced with Basalt FRP bars is compared to the flexural response of beams reinforced with either Carbon FRP or steel bars, but this time using similar axial stiffness value (EA ≈ 30 MN) of the reinforcement (i.e., 3T16B vs 2T12C and 2T10S). It is interesting to notice that Basalt and Carbon FRP-reinforced beams showed similar flexural response in terms of cracking moment and stiffness with slight variation in their ultimate capacities. This similarity was observed in both types of concrete compressive strengths. On top of that, both FRP-reinforced beams achieved higher moments than steel-reinforced beams.

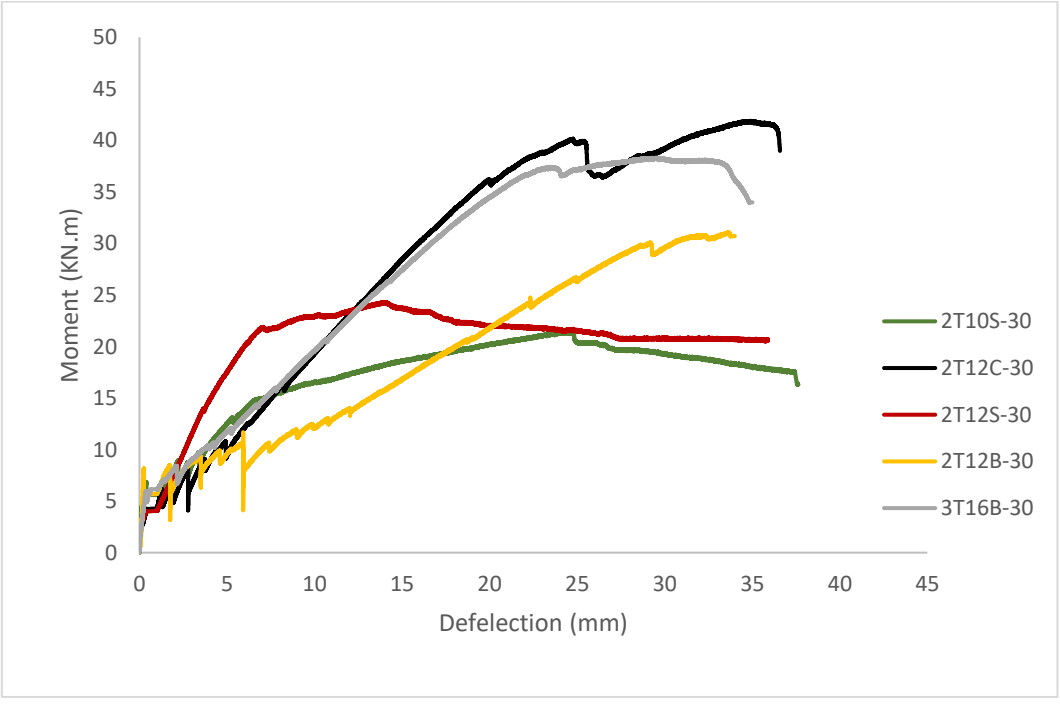

(a)

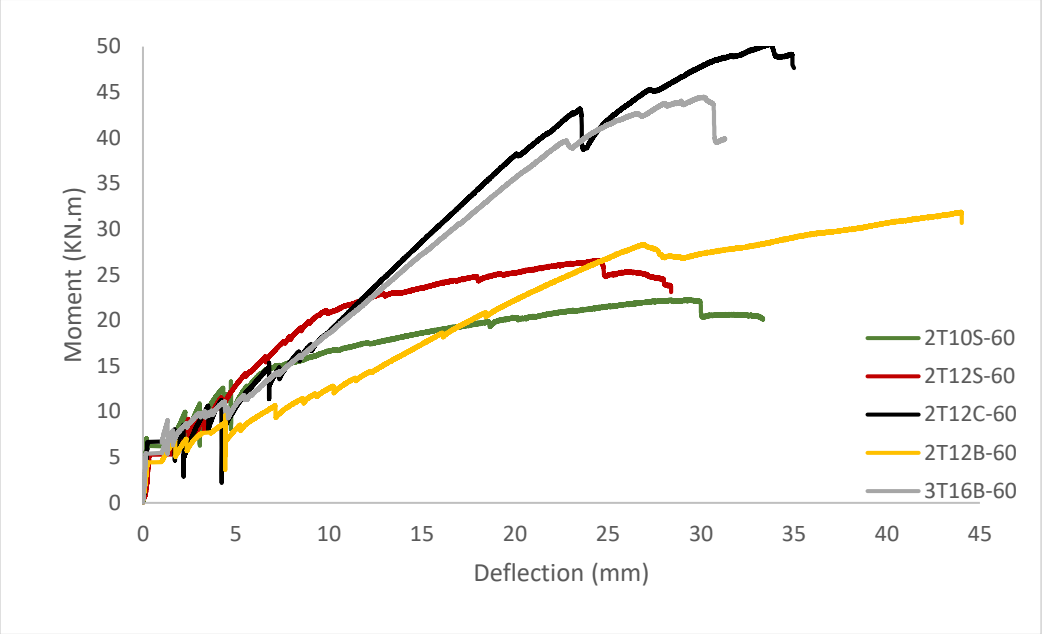

(b)

Figure 23: Moment vs Deflection for beams with BFRP, CFRP and Steel bars, (a) beams cast with f'_c = 30 MPa, (b) beams cast with f'_c = 60 MPa

Although it depends on the concrete strength and the modulus of rupture, the cracking moment values in the steel and CFRP-reinforced beams were very close. The BFRP-reinforced beams showed higher cracking moment except for the 3T16B-30 beam which showed a cracking moment value that is close to the steel and CFRP-reinforced beams. The experimental and the theoretical cracking moment values are summarized in Tables 12 and 13. As mentioned earlier, increasing the reinforcement ratio has no significant effect on the cracking moment value which confirms equations (14) and (15) in ACI440.1R-15 [1]. Likewise, changing the reinforcement type has no influence on the value of the cracking moment. Figures 15 and 16 shows the cracking patterns of the beams at service and at ultimate stages, respectively. The beams having similar axial stiffness (EA) showed close cracking behavior. Cracks start in the extreme tension fibers of the beams in the pure moment zone, then propagate to the top compression fibers until concrete crushing occurs. Beams having similar reinforcement ratio but different reinforcement type displayed similar cracking trend as shown in Figure 13b and 14b. However, the steel-reinforced beams showed smaller crack widths at higher load than the FRP-reinforced beams.

All beams showed similar pre-cracking behavior before the first crack. After the occurrence of the first crack, the behavior of the beams change depending on the

reinforcement type. For instance, the steel-reinforced beam showed higher strains than the FRP-reinforced beams due to the high modulus of elasticity of steel as shown in Figures 18a and 18b. The FRP-reinforced beams showed a typical linear behavior after cracking. However, the behavior of the steel beam has changed to inelastic after yielding of the steel bars. All beams showed major increase in the strain values after cracking. Tables 14 and 15 summarize the reinforcement strain and the concrete strain of the beams cast with concrete strength of 30 and 60 MPa, respectively. The reinforcement strain is measured at mid-span of the beam while the concrete strain is measured at the extreme compression fibers. The 3T16B-60 and 2T12C-60 beams showed similar reinforcement strain value of 0.0125 because both beams have similar axial stiffness (EA). In addition, although the 2T10S-60 beam has similar axial stiffness (EA) to the beams 3T16B-60 and 2T12C-60, the former beam showed similar strain behavior before cracking to the latter beams. However, following cracking, the behavior of the 2T10S-60 beam changed due to the yielding of the steel reinforcement. Consequently, the behavior of the beam changed from elastic to inelastic which allowed the beam to bear more deflection. Beams with similar reinforcement ratio of 2T12 bars showed different strains due to the different properties of the reinforcing bars.

FRP-reinforced beams experienced concrete crushing failure whereas the steel-reinforced concrete beams failed in steel yielding followed by crushing of concrete. Similar behavior was obtained by Abed et al. [20] and Elgabbas et al. [35]. As per the ACI440.1R-15, the beams reinforced with FRP bars shall be designed to fail in concrete crushing prior to FRP rupture. One the other hand, the typical failure for the steel-reinforced beams that is recommended by the ACI318 code is steel yielding to allow the beam to undergo to the inelastic behavior which is more ductile behavior, hence, the steel-reinforced beams are designed as under-reinforced ($\rho_s < \rho_b$) [37]. As a result, the strain in the steel reinforced beams reached an average value greater than 0.03 which proves that the steel bars have yielded prior reaching to ultimate compressive strain of 0.003. Regarding the beams reinforced with Basalt FRP and Carbon FRP bars, the concrete compressive strain reached ultimate with an average value of 0.0034 while the tensile strain the reinforcement bars is around an average of 0.0134 which is less than the ultimate tensile strain value. Figures 24 and 25 show the failure modes of the beams cast with concrete compressive strength of 30 and 60 MPa, respectively.

2T12C-30

2T10S-30

2T12S-30

Figure 24: Failure modes of concrete beams reinforced with CFRP and Steel bars, beams cast with f'_c=30 MPa

2T12C-60

2T10S-60

2T12S-60

Figure 25: Failure modes of concrete beams reinforced with CFRP and Steel bars, beams cast with f'_c=60 MPa

6.3 Analytical Prediction – Flexural Capacity

Tables 16 and 17 shows the experimental versus the theoretical moment capacity of beams cast with $f'c$ = 30 MPa and $f'c$ = 60 MPa, respectively. The theoretical moment capacity is calculated as per the moment equation (6) in chapter 4 specified by AC1440 for FRP-RC beams and ACI-318 for steel-RC beams. The FRP-reinforced beams are designed as over-reinforced to allow them to fail in concrete crushing as recommended by ACI440 code (see equations and procedures in section 4). Whereas, the steel-reinforced beams are designed as tension-controlled to undergo steel yielding. The experimental moment capacities of all the tested beams were higher than the predicted moment capacity by an approximate average value of 14%.

Table 16: Experimental vs theoretical moment for beams cast with f'_c=30 MPa

Beam	Experimental Moment Capacity (kN.m)	Theoretical Moment Capacity (kN.m)	Mu_{exp}/Mu_{th}
3T8B-30	23	20.5	1.12
2T10B-30	22.9	20.9	1.10
2T12-B-30	31.1	25.2	1.23
3T16B-30	38.3	37.0	1.04
2T12C-30	41.9	37.9	1.11
2T10S-30	21.4	16.1	1.33
2T12S-30	24.3	22.65	1.07

Table 17: Experimental vs theoretical moment capacity, beams cast with f'_c=60 MPa

Beam	Experimental Moment Capacity (kN.m)	Theoretical Moment Capacity (kN.m)	Mu_{exp}/Mu_{th}
3T8B-60	26	23.3	1.12
2T10B-60	24.7	23.7	1.04
2T12-B-60	31.9	28.8	1.11
3T16B-60	44.5	43.0	1.03
2T12C-60	50.4	44.2	1.13
2T10S-60	22.3	16.4	1.36
2T12S-60	26.6	23.1	1.15

6.4 Bond-dependent Coefficient (k_b)

The recommended value of the bond-dependent coefficient (k_b) is 1.4 as per ACI440.1R-15. Tables 18 and 19 provide the k_b values for all tested beams at different stages. The values are calculated at 33% of the maximum moment, 67% of the maximum moment and 0.7 mm crack width using equation (17). The value of k_b depends on the crack width, strain in the reinforcement and the spacing between the reinforcement. As the crack width increases, the value of k_b increases. On the other hand, while the strain in the reinforcement increases, the value of k_b decreases. In addition, the spacing of the reinforcement plays a major role in affecting the value of k_b. As the spacing between the reinforcement decreases, the value of k_b decrease.

As per Tables 18 and 19, all beams with three main reinforcing bars have lower value of k_b due to the small spacing between the bars. In addition, the table shows that majority of the values are less than or equal to 1 which indicates that FRP bars bond perfectly with concrete as strong as the steel bond with concrete. It can be understood from Tables 18 and 19 that the beams cast with concrete compressive strength = 60 MPa and the beams cast with f'_c = 30 MPa reported similar k_b values. The results show that the k_b values range from 0.51 to 1.1 with an average of 0.85 for the tested sand-coated FRP bars. The comparison confirms that the k_b value specified in ACI440 code amplify the crack widths of the tested beams and it is conservative.

Table 18: Bond-dependent Coefficient (k_b), beams cast with f'_c = 30 MPa

Beam ID	M_n Max	33% M_n	67% M_n	w=0.7	Mean
3T8B-30	23	0.51	0.76	0.85	0.71
2T10B-30	22.9	0.88	0.69	0.69	0.75
2T12B-30	31.1	0.94	0.99	1.07	1.00
3T16B-30	38.3	0.67	1.03	0.99	0.90
2T12C-30	41.9	0.99	0.99	0.98	0.99
2T10S-30	21.4	0.49	0.92	0.99	0.80
2T12S-30	24.3	0.82	0.99	0.98	0.93

Table 19: Bond-dependent Coefficient (k_b), beams cast with f'_c = 60 MPa

Beam ID	M_n Max	33% M_n	67% M_n	w=0.7	Mean
3T8B-60	26	1.04	0.69	0.69	0.81
2T10B-60	24.7	0.74	1.10	0.97	0.94
2T12B-60	31.9	0.76	1.09	0.80	0.88
3T16B-60	44.5	0.54	0.68	0.88	0.70
2T12C-60	50.4	0.66	0.97	0.78	0.80
2T10S-60	22.3	0.63	0.94	0.96	0.84
2T12S-60	26.6	0.99	0.77	0.82	0.86

Chapter 7: Summary and Conclusions

Several materials have been used as internally reinforcing rebars for structural concrete members. The experimental program of this research is conducted to investigate the effects of varying reinforcement ratios and reinforcement axial stiffness on the flexural response of concrete beams reinforced longitudinally with Basalt Fiber Reinforced Polymers (BFRP) bars, considering two different concrete compressive strengths. In addition, the behavior of BFRP bars when used as main reinforcement are compared with CFRP and steel bars. In reference to the results obtained from the experimental program, several conclusions and observations are drawn and listed below:

1) Increasing the reinforcement ratio of the BFRP-reinforced beams enhance the load carrying capacity as well as the moment capacity of the concrete beams. The percentage increase in the moment capacity confirms the trend of the moment equation provided by the ACI440.1R-15 guidelines.
2) Increasing the reinforcement ratio has no effect on increasing the cracking moment of the beams. This confirms the ACI440.1R-15 equations that the cracking moment depends on the modulus of rupture and concrete strength.
3) Increasing the reinforcement ratio has no impact on the crack width values. However, increasing the number of bars reduces the spacing between the bars which reduces the crack widths.
4) BFRP-reinforced beams that have similar axial stiffness (EA) showed comparable flexural response with very close moment capacities.
5) FRP-reinforced beams failed in concrete crushing prior reaching the ultimate strain in the reinforcing bars. While the steel-reinforced beams failed in steel yielding followed by concrete crushing.
6) Among all the beams, the CFRP-reinforced beams reached the highest moment capacity due to the high value of the tensile strength of the reinforcing bars.
7) All beams exhibited similar pre-cracking behavior. Subsequent to cracking, the stiffness of the beams reduces significantly, and the reinforcement start getting engaged in the load carrying capacity undergoing a sudden increase in the strain values.

8) The bond-dependent (k_b) factor is directly proportional to the crack width. However, it is indirectly proportional to the reinforcement strain and the spacing of the reinforcing bars.
9) The average bond dependent coefficient (k_b) value was obtained to be less than 1.0. Increasing the compressive strength has almost no effect on the value of k_b. future studies are recommended to investigate this matter further.
10) The BFRP-reinforced beams showed similar behavior to the CFRP-reinforced beams which supports that the BFRP bars can be used in the similar applications of other FRP reinforcing bars.
11) Future studies could be made by developing a nonlinear finite element model to validate the results obtained from the experimental tests and compare them in terms of the load carrying capacity, the cracking behavior and the failure mode.

References

[1] ACI Committee 440, *Guide for the design and construction of concrete reinforced with FRP bars*. Farmington Hills, MI: American Concrete Institute, 2015.

[2] L. C. Bank, *Composites for Construction*. John Wiley & Sons,Hoboken, p.560 New Jersey, 2006.

[3] Z. Dong, G. Wu, B. Xu, X. Wang, and L. Taerwe, "Bond durability of BFRP bars embedded in concrete under seawater conditions and the long-term bond strength prediction," *Materials & Design*, vol. 92, pp. 552–562, 2016.

[4] S. Alhamad, Y. A. Banna, A. A. Osman, J. Mouthassseeb, S. Abdalla and F. Abed, "Effect of shear span-to-depth ratio on the shear behavior of BFRP-RC deep beams," *2017 International Conference on Advances in Sustainable Construction Materials & Civil Engineering Systems (ASCMCES),* 2017.

[5] A. T. H. Altalmas, "Durability Study on the Bond Strength of Basalt Fiber-Reinforced Polymer (BFRP) Bars," Masterthesis, American University of Sharjah, Sharjah, 2014.

[6] S. Abedi, "Evaluation of the bond and tensile strength of GFRP bars exposed to harsh environment," Master thesis, American University of Sharjah, Sharjah, 2014.

[7] B. Columbia, M. East, and M. Vesuvius, *Advanced concrete for use in civil engineering*, Woodhead, p 376, Cambridge, 2006.

[8] M. M. Rafi, A. Nadjai, and F. Ali, "Experimental Testing of Concrete Beams Reinforced with Carbon FRP Bars," *Journal of Composite Materials*, vol. 41, no. 22, pp. 2657–2673, 2007.

[9] F. Abed, H. El-Chabib, and M. AlHamaydeh, "Shear characteristics of GFRP-reinforced concrete deep beams without web reinforcement," *Journal of Reinforced Plastics and Composites*, vol. 31, no. 16, pp. 1063–1073, 2012.

[10] M. Theriault, B. Benmokrane, "Effects of FRP Reinforcement Ratio and Concrete Strength on Flexural Behavior of Concrete Beams," *Journal of Composites for Construction*, vol. 2, no. 2, pp. 7–16, 1998.

[11] A. E. Refai, F. Abed, and A. Al-Rahmani, "Structural performance and serviceability of concrete beams reinforced with hybrid (GFRP and steel) bars,"

Construction and Building Materials, vol. 96, pp. 518–529, 2015.

[12] A. Sagher and F. Abed, “Finite element parametric study of the shear behavior of GFRP-RC short beams,” *2017 7th International Conference on Modeling, Simulation, and Applied Optimization (ICMSAO)*, 2017.

[13] M. N. Habeeb and A. F. Ashour, "Flexural Behavior of Continuous GFRP Reinforced Concrete Beams," *Journal of Composites for Construction*, vol. 12, no. 2, pp. 115-124, 2008.

[14] H. Zhang, L. He, and G. Li, “Bond failure performances between near-surface mounted FRP bars and concrete for flexural strengthening concrete structures,” *Engineering Failure Analysis*, vol. 56, pp. 39–50, 2015.

[15] B. Abdul-Salam, A. S. Farghaly, and B. Benmokrane, “Mechanisms of shear resistance of one-way concrete slabs reinforced with FRP bars,” *Construction and Building Materials*, vol. 127, pp. 959–970, 2016.

[16] V. Calvet, M. Valcuende, J. Benlloch, and J. Cánoves, “Influence of moderate temperatures on the bond between carbon fibre reinforced polymer bars (CFRP) and concrete,” *Construction and Building Materials*, vol. 94, pp. 589–604, 2015.

[17] P. Escórcio and P. M. França, “Experimental study of a rehabilitation solution that uses GFRP bars to replace the steel bars of reinforced concrete beams,” *Engineering Structures*, vol. 128, pp. 166–183, 2016.

[18] A. El-Nemr, E. A. Ahmed, C. Barris, and B. Benmokrane, “Bond-dependent coefficient of glass- and carbon-FRP bars in normal- and high-strength concretes,” *Construction and Building Materials*, vol. 113, pp. 77–89, 2016.

[19] A. Al-Tamimia, F. H. Abed, and A. Al-Rahmani, “Effects of harsh environmental exposures on the bond capacity between concrete and GFRP reinforcing bars,” *Advances in concrete construction*, vol. 2, no. 1, pp. 1–11, 2014.

[20] F. Abed and A. R. Alhafiz, “Effect of basalt fibers on the flexural behavior of concrete beams reinforced with BFRP bars,” *Composite Structures*, vol. 215, pp. 23–34, 2019.

[21] A. E. Refai and F. Abed, “Concrete Contribution to Shear Strength of Beams Reinforced with Basalt Fiber-Reinforced Bars,” *Journal of Composites for Construction*, vol. 20, no. 4, p. 150, 2016.

[22] A. Altalmas, A. E. Refai, and F. Abed, “Bond degradation of basalt fiber-reinforced polymer (BFRP) bars exposed to accelerated aging conditions,” *Construction and Building Materials*, vol. 81, pp. 162–171, 2015.

[23] M. Hassan, B. Benmokrane, A. Elsafty, and A. Fam, “Bond durability of basalt-fiber-reinforced-polymer (BFRP) bars embedded in concrete in aggressive environments,” *Composites Part B: Engineering*, vol. 106, pp. 262–272, 2016.

[24] F. Elgabbas, E. A. Ahmed, and B. Benmokrane, “Physical and mechanical characteristics of new basalt-FRP bars for reinforcing concrete structures,” *Construction and Building Materials*, vol. 95, pp. 623–635, 2015.

[25] F. Elgabbas, P. Vincent and B. Benmokrane, “Experimental testing of basalt-fiber-reinforced polymer bars in concrete beams,” *Composites Part B: Engineering*, vol. 91, pp. 205-2018, 2016.

[26] D. Tomlinson and A. Fam, “Performance of Concrete Beams Reinforced with Basalt FRP for Flexure and Shear,” *Journal of Composites for Construction*, vol. 19, no. 2, p. 150, 2015.

[27] H. Wang and A. Belarbi, “Ductility characteristics of fiber-reinforced-concrete beams reinforced with FRP rebars,” *Construction and Building Materials*, vol. 25, no. 5, pp. 2391–2401, 2011.

[28] A. E. Refai, F. Abed, and A. Altalmas, “Bond Durability of Basalt Fiber–Reinforced Polymer Bars Embedded in Concrete under Direct Pullout Conditions,” *Journal of Composites for Construction*, vol. 19, no. 5, p. 1-11, 2015.

[29] F. Abed and A. R. Alhafiz, “Finite element simulation of the flexural behavior of BFRP-FRC beams,” *2018 Advances in Science and Engineering Technology International Conferences (ASET)*, 2018.

[30] A. El Refai, M.A. Ammar, and R. Masmoudi, “Bond performance of basalt fiber-reinforced polymer bars to concrete,” *Journal of Composites for Construction*, vol. 19, no. 3, p. 150-166, 2014.

[31] F. H. Abed, A. Al-Rahmani, and A. H. Al-Rahmani, “Finite element simulations of the shear capacity of GFRP-reinforced concrete short beams,” *2013 5th International Conference on Modeling, Simulation and Applied Optimization (ICMSAO)*, 2013.

[32] F. H. Abed, A. Al-Rahmani, and A. H. Al-Rahmani, “Finite element simulations

of the shear capacity of GFRP-reinforced concrete short beams," *2013 5th International Conference on Modeling, Simulation and Applied Optimization (ICMSAO)*, 2013.

[33] A. Al-Rahmani and F. H. Abed, "Numerical investigation of hybrid FRP reinforced beams," *2013 5th International Conference on Modeling, Simulation and Applied Optimization (ICMSAO)*, 2013.

[34] F. S. Makarem and F. Abed, "Nonlinear finite element modeling of dynamic localizations in high strength steel columns under impact," *International Journal of Impact Engineering*, vol. 52, pp. 47–61, 2013.

[35] F. Elgabbas, E. A. Ahmed, and B. Benmokrane, "Flexural Behavior of Concrete Beams Reinforced with Ribbed Basalt-FRP Bars under Static Loads," *Journal of Composites for Construction*, vol. 20, no. 4, p. 230, 2016.

[36] P. K. Mallick, *Composites Engineering Handbook*. New York: M. Dekker, 1997.

[37] *Building code requirements for reinforced concrete and commentary*, American Concrete Institute (ACI) Committee 318, Farmington Hills, MI, 2011.

[38] F. Abed and F. Makarem, "Comparisons of Constitutive Models for Steel Over a Wide Range of Temperatures and Strain Rates," *Journal of Engineering Materials and Technology*, vol. 134, no. 2, p. 1-10, 2012.

[39] F. H. Abed, S. I. Ranganathan, and M. A. Serry, "Constitutive modeling of nitrogen-alloyed austenitic stainless steel at low and high strain rates and temperatures," *Mechanics of Materials*, vol. 77, pp. 142–157, 2014.

Vitae

Mustafa Al-Mimar was born in 1991, in Baghdad, Iraq. Mustafa graduated from National Charity School (NCS) in 2009. After that, he joined the American University of Sharjah to pursue a Bachelor of Science degree in Civil Engineering. He completed his undergraduate studies in June 2014.

He started his career in a local consultant company, QHC Architects and Engineers, as a junior structural engineer in August 2014. A year later, he started to pursue a MSc. degree in Civil Engineering at AUS; he worked as a part-time Graduate Teaching Assistant.

During his master's studies, Mustafa was interested in the field of strengthening of RC structures using composites. In October 2016, he joined Structural Technologies, a reputable reinforced concrete strengthening and repair specialist, as a Structural Engineer until the present time.